Chapter 9

https://doi.org/10.32685/pub.esp.37.2019.09
Published online 26 November 2020

Cenozoic Marine Carbonate Systems of Colombia

Juan Carlos SILVA–TAMAYO[1]*, Daniel RINCÓN–MARTÍNEZ[2], Lina M. BARRIOS[3], Juan C. TORRES–LASSO[4], and Chixel OSORIO–ARANGO[5]

1 director.testlabgeoambiental@gmail.com
CEO at Testlab Geoambiental
Testlab Laboratorio Alimentos y Aguas S.A.S.
Research Group One–Health
Calle 45D n.° 60–16
Medellín, Colombia

2 daniel.rincon@ecopetrol.com.co
Ecopetrol S.A
Instituto Colombiano del Petróleo
Centro de Innovación y Tecnología
Bucaramanga, Santander, Colombia

3 lina.barrios@mmu.ac.uk
Manchester Metropolitan University
School of Science and the Environment
Environment and Ecology Research Centre–EERC
Chester St, Manchester, M1 5GD, United Kingdom

4 juan.lasso.col@furg.br
Universidade Federal do Rio Grande
Instituto de Geociências
Rio Grande, Rio Grande du Sul, Brasil
Universidad de Caldas
Departamento de Geología
Manizales, Colombia

5 cyosorio@unal.edu.co
Smithsonian Tropical Research Institute
Panamá, Panamá
Universidad Nacional de Colombia
Sede Medellín
Departamento de Ingeniería Geológica
Medellín, Colombia

* Corresponding author

Abstract In this chapter, we report existing and new lithostratigraphic information and Sr–isotope chemostratigraphic ages of several Cenozoic marine carbonate successions deposited within numerous Colombian basins. This information is used to link main changes in the shallow marine carbonate factory to regional environmental/tectonic events in the tropical SE Circum–Caribbean. Our results and the available literature show that during the Eocene – early Oligocene transition, carbonate successions developed along the Alta Guajira (Macarao Formation) and the San Jacinto (Toluviejo and Arroyo de Piedra Formations) Basins, northern Colombia. These successions, which deposited along rimmed carbonate banks, mostly display heterozoan biotic associations, dominated by red algae and large benthic foraminifera. The development of this carbonate factory occurred during an interval of hothouse conditions through which mesotrophic and oligophotic marine conditions predominated. During the late Oligocene, carbonate sedimentation occurred along the Alta Guajira Basin (Siamana Formation), Lower Magdalena Valley Basin (Cicuco Limestones of the Ciénaga de Oro Formation), and Western Cordillera of Colombia (Vijes Formation). Predominant mesotrophic conditions resulted in the coexistence of mixed photozoan–heterozoan biotic associations and the development of patchy coral reefs along the predominantly siliciclastic continental shelves. During the early Miocene, carbonate deposition was absent in most of the Colombian sedimentary basins and was restricted to the Alta Guajira Basin, where photozoan biotic associations dominated the emerging rimmed coral–dominated carbonate platforms attached to the continental shelves. The change in coral reef architecture along the Alta Guajira Basin coincides with the onset of a global climate optimum and of local marine oligotrophic and euphotic conditions. The replacement of photozoan by heterozoan biotic associations in the Alta Guajira Basin during the middle Miocene likely resulted from the return to mesotrophic/oligophotic conditions due to the enhancement of the sediment supply to the Caribbean as the docking of the Panamá Block to northern South America reached its acme. The enhanced sediment supply to the Caribbean decreased the occurrence of well–developed reefs along the Caribbean region of Colombia (continental) during the late Miocene and Pliocene. This decrease, which parallels global trends, is only interrupted by the deposition of the late Miocene San Andrés and Pleistocene San Luis Formations (Los Cayos Basin), where photozoan

Citation: Silva–Tamayo, J.C., Rincón–Martínez, D., Barrios, L.M., Torres–Lasso, J.C. & Osorio–Arango, C. 2020. Cenozoic marine carbonate systems of Colombia. In: Gómez, J. & Mateus–Zabala, D. (editors), The Geology of Colombia, Volume 3 Paleogene – Neogene. Servicio Geológico Colombiano, Publicaciones Geológicas Especiales 37, p. 249–282. Bogotá. https://doi.org/10.32685/pub.esp.37.2019.09

biotic associations prevailed, and the Pleistocene La Popa Formation (San Jacinto Basin), which displays mixed photozoan–heterozoan biotic associations.
Keywords: *Colombia, Cenozoic, stratigraphy, carbonate sedimentology, photozoan carbonate, heterozoan carbonate, environmental archives.*

Resumen En este capítulo reportamos información litoestratigráfica existente y nueva y edades quimioestratigráficas de isótopos de Sr de varias sucesiones carbonáticas marinas del Cenozoico que se depositaron en diferentes cuencas colombianas. Esta información se usa para relacionar los principales cambios en las fábricas de carbonatos marinos poco profundos con eventos ambientales/tectónicos regionales en el Caribe suroriental. Nuestros resultados y la literatura disponible muestran que durante la transición Eoceno–Oligoceno temprano se desarrollaron sucesiones de carbonatos en las cuencas Alta Guajira (Formación Macarao) y San Jacinto (formaciones Toluviejo y Arroyo de Piedra), al norte de Colombia. Estas sucesiones, que se depositaron en bancos bordeados por carbonatos, presentan en su mayoría asociaciones biológicas heterozoarias, dominadas por algas rojas y foraminíferos bentónicos grandes. El desarrollo de esta fábrica carbonática tuvo lugar durante un intervalo de invernadero a través del cual predominaron condiciones marinas mesotróficas y oligofóticas. Durante el Oligoceno tardío, la sedimentación de carbonatos ocurrió en la Cuenca Alta Guajira (Formación Siamana), Cuenca del Valle Inferior del Magdalena (Calizas del Cicuco de la Formación Ciénaga de Oro) y cordillera Occidental colombiana (Formación Vijes). Las condiciones mesotróficas predominantes dieron como resultado la coexistencia de asociaciones biológicas mixtas fotozoarias–heterozoarias y el desarrollo de arrecifes de coral irregulares a lo largo de las plataformas continentales predominantemente siliciclásticas. En el Mioceno temprano, el depósito de carbonatos estuvo ausente en la mayoría de cuencas sedimentarias colombianas y se restringió a la Cuenca Alta Guajira, donde las asociaciones biológicas fotozoarias dominaron las plataformas carbonáticas emergentes bordeadas por corales unidas a las plataformas continentales. El cambio en la arquitectura de los arrecifes de coral a lo largo de la Cuenca Alta Guajira coincide con el inicio de un clima global óptimo y de condiciones marinas locales oligotróficas y eufóticas. El reemplazo de asociaciones biológicas fotozoarias por asociaciones heterozoarias en la Cuenca Alta Guajira durante el Mioceno medio probablemente se debió al regreso a las condiciones mesotróficas/oligofóticas debido al aumento en el aporte de sedimentos al Caribe a medida que la acreción del Bloque de Panamá al norte de Suramérica alcanzó su auge. Este aumento en la sedimentación redujo la aparición de arrecifes bien desarrollados a lo largo de la región Caribe de Colombia (continental) durante el Mioceno tardío y Plioceno. Esta disminución, que es paralela a las tendencias globales, solo es interrumpida por el depósito de las formaciones San Andrés del Mioceno tardío y San Luis del Pleistoceno (Cuenca Los Cayos), donde asociaciones biológicas fotozoarias prevalecieron, y de la Formación La Popa del Pleistoceno (Cuenca San Jacinto), que muestra predominio de asociaciones mixtas fotozoarias–heterozoarias.
Palabras clave: *Colombia, Cenozoico, estratigrafía, sedimentología de carbonatos, carbonato de fotozoarios, carbonato de heterozoarios, archivos ambientales.*

1. Introduction

The marine carbonate sedimentary factory comprises the production, deposition, and early modification of carbonate sediments (James & Jones, 2016). There are two main marine carbonate factories: The benthic carbonate factory that develops on the seafloor, and the pelagic carbonate factory that develops in the water column (Figure 1). Such carbonate factories continuously produce carbonate sediments, which exhibit wide range of grain sizes and can be produced inorganically or biologically or by a combination of both (James & Jones, 2016).

Tropical marine carbonate factories are restricted to the latitudinal range between 15° N and 15° S, an area characterized by a warm sea surface temperature, low nutrient level, high at-

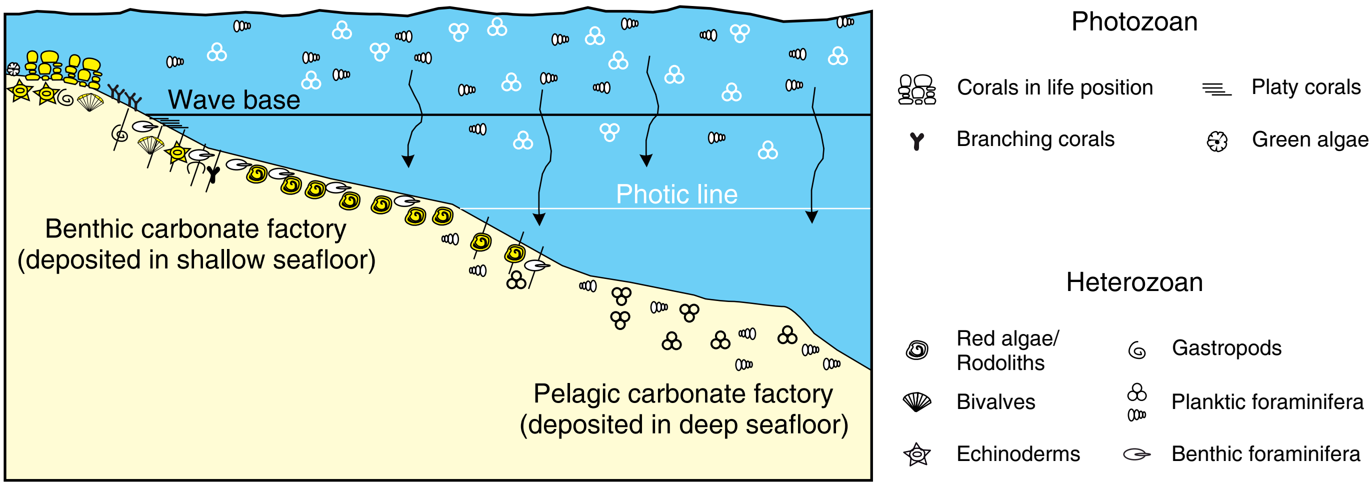

Figure 1. Main tropical marine biogenic carbonate producers and carbonate factories with respect to water depth.

mospheric humidity, and heavy rainfall. Seasonal fluctuations in both temperature and precipitation also influence the marine currents, clastic nutrient input, and freshwater discharges into the marine basins (Lockwood, 1974). Although the warm ocean temperature in tropical areas is the main mechanism promoting carbonate production, additional factors such as chemical saturation, salinity, turbidity, nutrient availability, and tectonic activity not only control such production on short time scales but also influence the type of carbonate factories (Budd, 2000; Frost, 1977; Johnson et al., 2008, 2009; Klaus et al., 2011; Mutti et al., 2005; Renema et al., 2016; Wilson, 2002, 2008, 2012, 2015).

Carbonate–secreting organisms account for most of the carbonate production of tropical marine carbonate factories. The occurrence of different types of carbonate producers and, thus, the type of carbonate factory depends on diverse environmental factors, i.e., light penetration, water salinity, nutrient availability, oxygen levels, and temperature (James & Jones, 2016; Wilson, 2012). Photozoans such as green calcareous algae, symbiotic larger benthic foraminifera (LBF), scleractinian corals, and siliceous sponges, which are organisms that depend on light to produce their own food by photosynthesis, constitute the main tropical carbonate factory (James & Jones, 2016; Wilson, 2012). The photozoan carbonate factory occurs in tropical marine areas characterized by oligotrophic (low nutrients), euphotic (highly illuminated), and warm ocean waters. The heterozoan carbonate factory consists of heterotrophic organisms, such as bryozoans, brachiopods, echinoderms, mollusks, azooxanthellate corals, and calcareous red algae. While calcareous red algae are not heterotrophs, they are common components in these carbonates. Although the heterozoan carbonate factory typically occurs in temperate regions, it may occur in tropical marine areas, where dimmed (euphotic–aphotic), moderate–to–high nutrient (mesotrophic, eutrophic), and cold ocean waters prevail (Figures 2, 3). Unlike the photozoan biotic associations, the heterozoan biotic associations are highly resistant to low oxygen conditions and may survive and adapt to variable salinity conditions (Figure 4; James & Jones, 2016; Wilson, 2012).

While much has been learned from living systems, many questions remain unanswered concerning how prehistoric events shaped ancient shallow marine carbonate factories in the tropical oceans (Wilson, 2012). Although on longer time–scales, global environmental/climatic events, biological evolution, geodynamics, and paleogeographic changes seem to have played important roles in the evolution of Cenozoic tropical carbonate factories, it has been observed that local parameters may play an overriding role that can mask the global signals. Therefore, it is necessary to understand regional variability before determining global implications (Wilson, 2012).

In this chapter, we compile published and report new lithostratigraphic and biostratigraphic information, as well as Sr–isotope chemostratigraphic data from several shallow marine Cenozoic carbonates successions from western and northern Colombia, including the Arroyo de Piedra, Toluviejo, Vijes, Macarao, Siamana, Ciénaga de Oro (Cicuco Limestones), San Andrés, and La Popa Formations (Figures 5, 6). This information is used to better constrain their carbonate factories, depositional age, and depositional settings. It is also used to investigate spatial and temporal changes in the shallow marine carbonate systems and ultimately relate such changes to climatic, environmental, and tectonic events.

2. Materials and Methods

The lithostratigraphic information for carbonates from the Arroyo de Piedra, Toluviejo, Siamana, Ciénaga de Oro, San Andrés, and La Popa Formations have been reported elsewhere (Ortiz & Niño, 1999; Ortiz et al., 1998; Reyes et al., 2009; Rosero et al., 2014; Salazar–Franco et al., 2016; Silva–Tamayo et al., 2017). In this chapter, we present new lithostratigraphic information from the Macarao and Vijes Formations. The car-

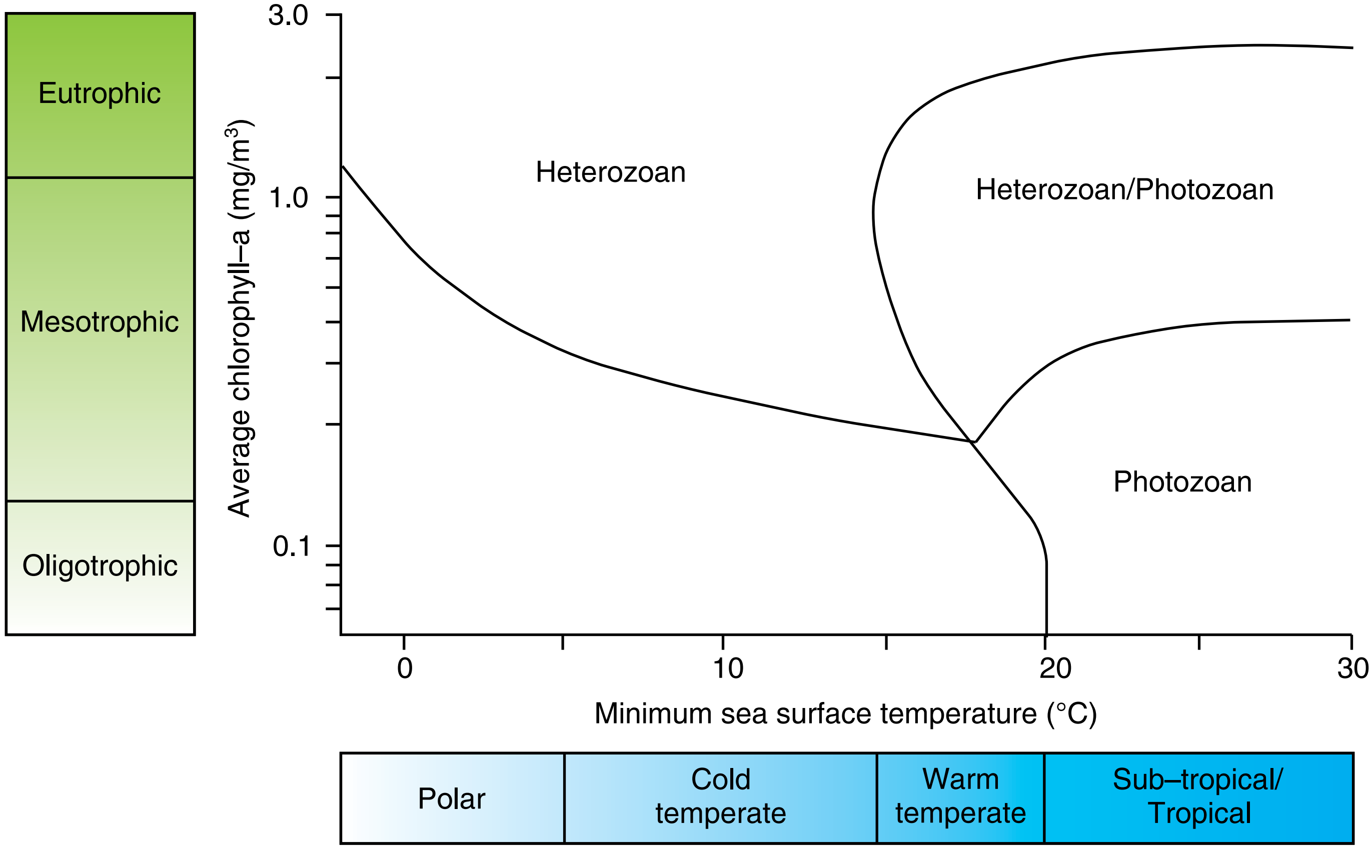

Figure 2. Variations in marine biogenic carbonate producers and carbonate factories with respect to nutrient levels and seawater temperature (James & Jones, 2016).

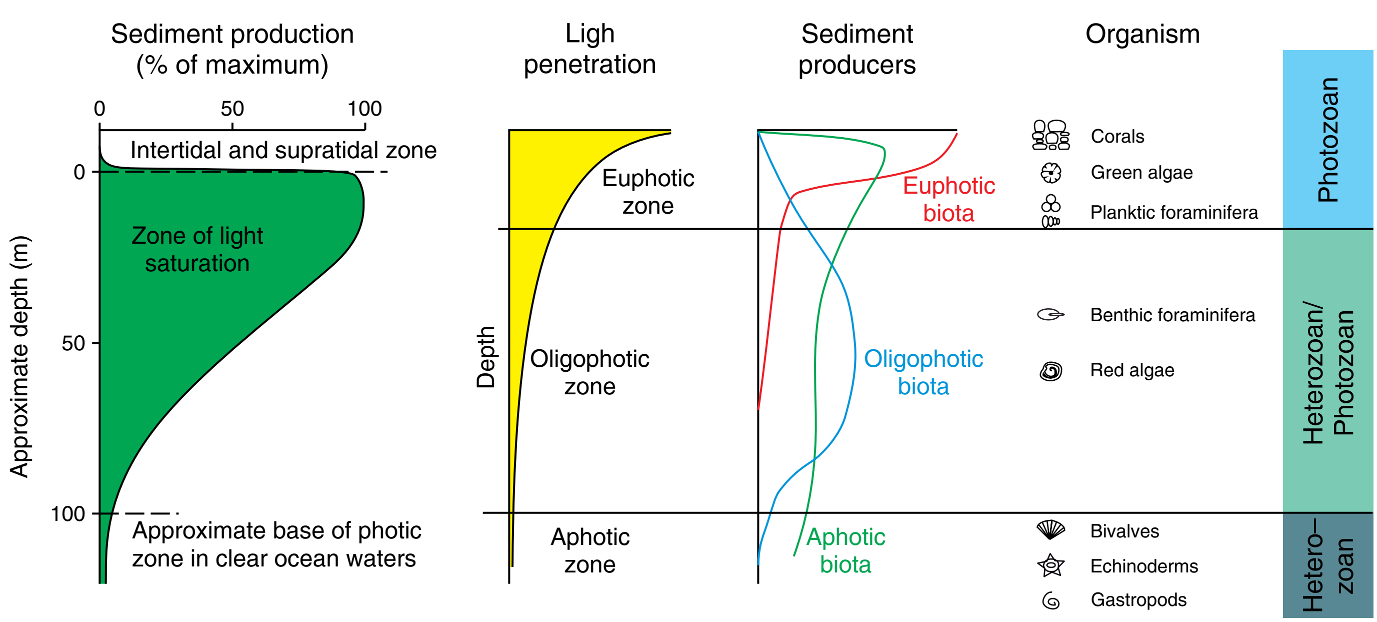

Figure 3. Variations in marine biogenic carbonate producers and carbonate factories with respect to light penetration and light saturation (James & Jones, 2016).

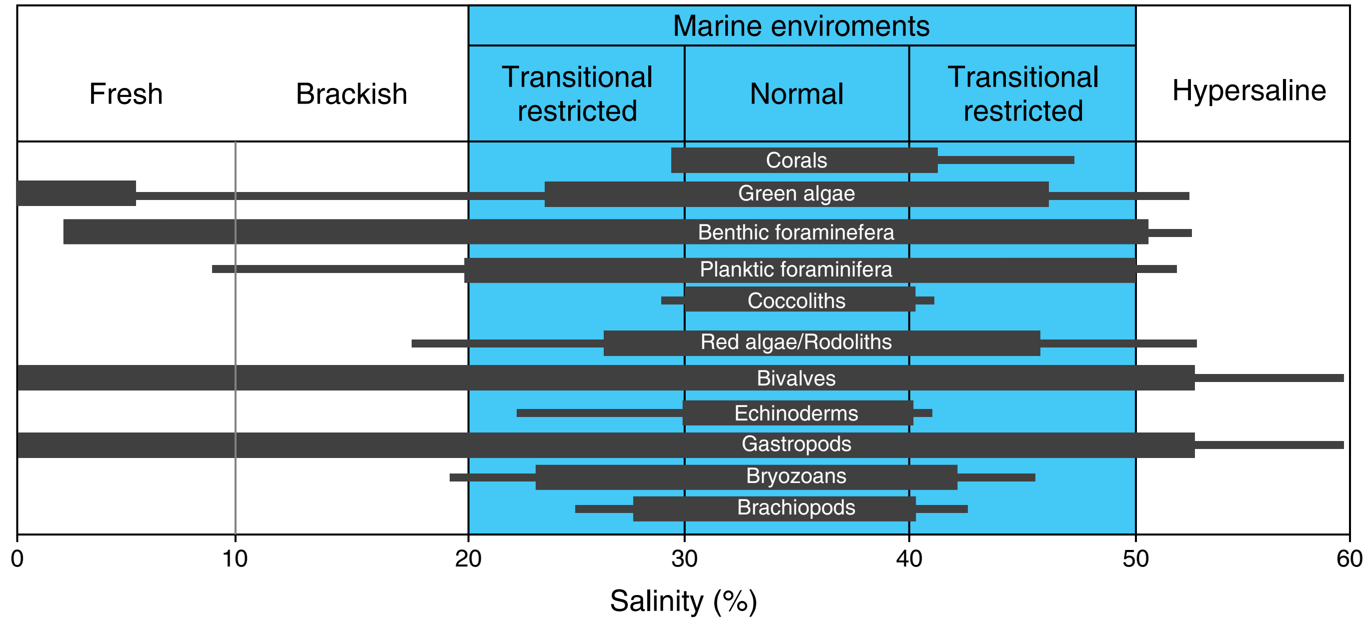

Figure 4. Variations in the occurrence of different marine carbonate producers with respect to salinity (James & Jones, 2016).

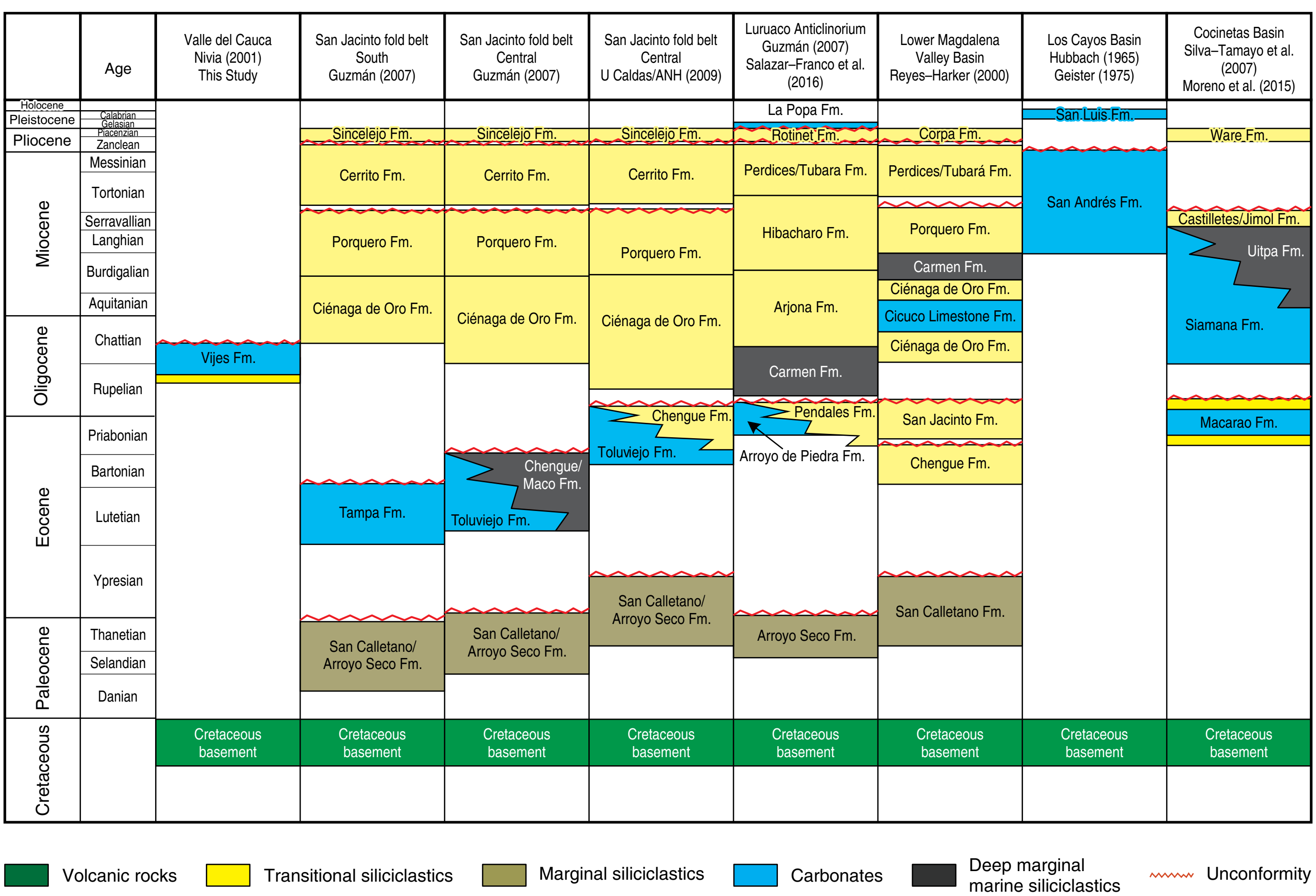

Figure 5. Litho and chronostratigraphic chart of the studied basins.

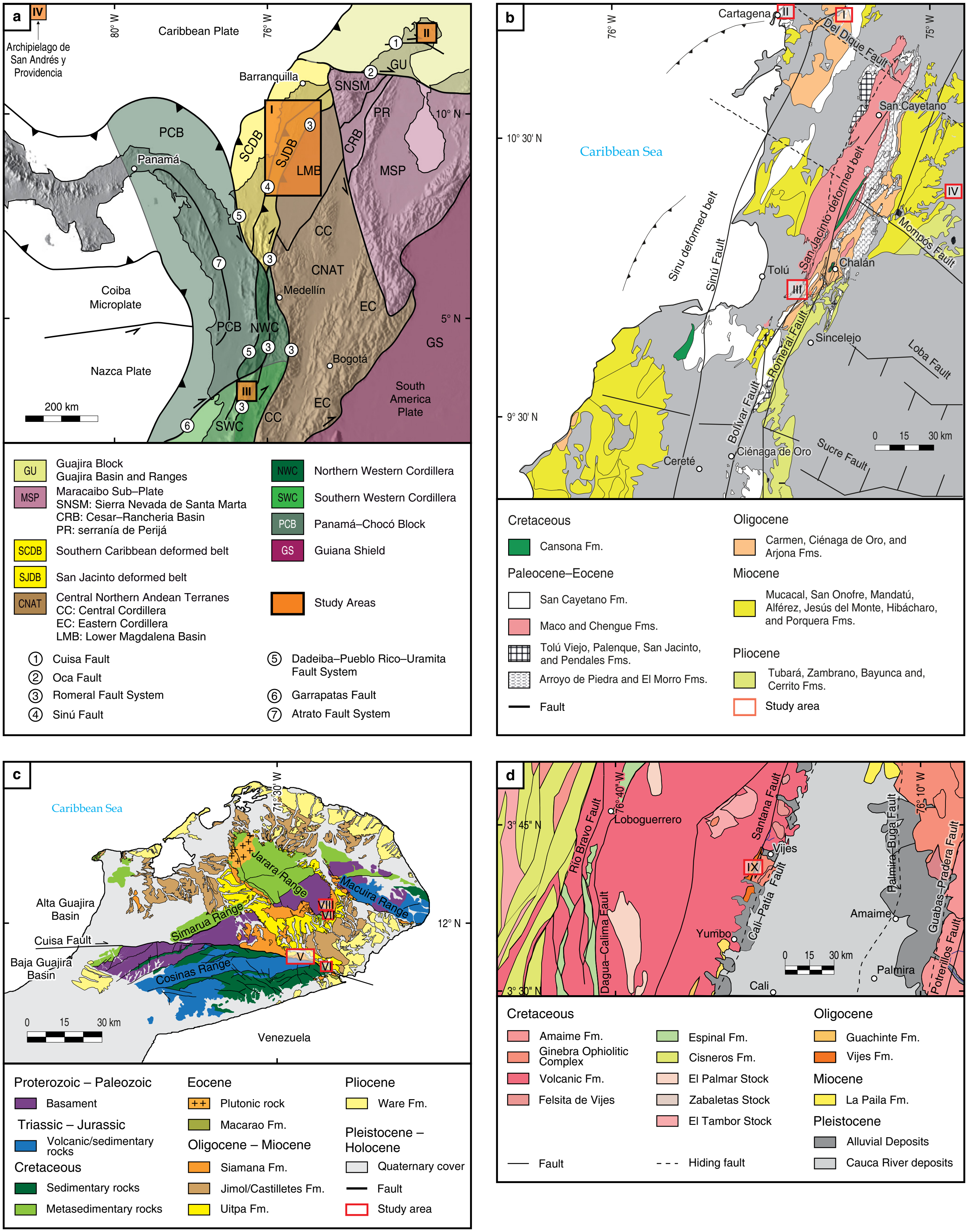
a
IV
Archipielago de San Andrés y Providencia
80° W
76° W
Caribbean Plate
II
GU
Barranquilla
SNSM
PR
10° N
CRB
MSP
PCB
Panamá
SCDB
SJDB
LMB
CC
CNAT
Coiba Microplate
Medellín
EC
5° N
PCB
NWC
GS
Nazca Plate
Bogotá
South America Plate
200 km
III
SWC
CC
EC
GU Guajira Block
Guajira Basin and Ranges
MSP Maracaibo Sub–Plate
SNSM: Sierra Nevada de Santa Marta
CRB: Cesar–Rancheria Basin
PR: serranía de Perijá
SCDB Southern Caribbean deformed belt
SJDB San Jacinto deformed belt
CNAT Central Northern Andean Terranes
CC: Central Cordillera
EC: Eastern Cordillera
LMB: Lower Magdalena Basin
NWC Northern Western Cordillera
SWC Southern Western Cordillera
PCB Panamá–Chocó Block
GS Guiana Shield
Study Areas
1 Cuisa Fault
2 Oca Fault
3 Romeral Fault System
4 Sinú Fault
5 Dadeiba–Pueblo Rico–Uramita Fault System
6 Garrapatas Fault
7 Atrato Fault System
b
76° W
75° W
Cartagena
II
I
Del Dique Fault
San Cayetano
10° 30' N
Caribbean Sea
IV
San Jacinto deformed belt
Mompos Fault
Sinu deformed belt
Sinú Fault
Tolú
Chalán
III
Romeral Fault
Sincelejo
Loba Fault
9° 30' N
Bolívar Fault
Ciénaga de Oro
Sucre Fault
Cereté
0 15 30 km
Cretaceous
Cansona Fm.
Paleocene–Eocene
San Cayetano Fm.
Maco and Chengue Fms.
Tolú Viejo, Palenque, San Jacinto, and Pendales Fms.
Arroyo de Piedra and El Morro Fms.
Fault
Oligocene
Carmen, Ciénaga de Oro, and Arjona Fms.
Miocene
Mucacal, San Onofre, Mandatú, Alférez, Jesús del Monte, Hibácharo, and Porquera Fms.
Pliocene
Tubará, Zambrano, Bayunca and, Cerrito Fms.
Study area
c
Caribbean Sea
71° 30' W
Jarara Range
Macuira Range
Alta Guajira Basin
VII
VI
12° N
Simarua Range
Cuisa Fault
Baja Guajira Basin
V
VI
Cosinas Range
0 15 30 km
Venezuela
Proterozoic – Paleozoic
Basament
Triassic – Jurassic
Volcanic/sedimentary rocks
Cretaceous
Sedimentary rocks
Metasedimentary rocks
Eocene
Plutonic rock
Macarao Fm.
Oligocene – Miocene
Siamana Fm.
Jimol/Castilletes Fm.
Uitpa Fm.
Pliocene
Ware Fm.
Pleistocene – Holocene
Quaternary cover
Fault
Study area
d
3° 45" N
76° 40" W
Loboguerrero
Río Bravo Fault
Santana Fault
Vijes
IX
Fault
Buga Fault
Palmira
76° 10" W
Potrerillos Fault
Guabas–Pradera Fault
Amaime
Dagua–Calima Fault
Yumbo
Cali–Patía
0 15 30 km
Palmira
3° 30" N
Cali
Cretaceous
Amaime Fm.
Ginebra Ophiolitic Complex
Volcanic Fm.
Felsita de Vijes
Espinal Fm.
Cisneros Fm.
El Palmar Stock
Zabaletas Stock
El Tambor Stock
Oligocene
Guachinte Fm.
Vijes Fm.
Miocene
La Paila Fm.
Pleistocene
Alluvial Deposits
Cauca River deposits
Fault
Hiding fault

←

Figure 6. (a) Tectonic map of Colombia (after Cediel et al., 2003). Orange squares represent the areas where Cenozoic marine carbonates occur: (I) SJDB; (II) Alta Guajira Basin; (III) Western Cordillera of Colombia; (IV) Los Cayos Basin. **(b)** Geologic map of the San Jacinto Basin (after Bermúdez et al., 2009). Roman numbers represent the locations of the stratigraphic sections reported in this study: (I) Luruaco Anticlinorium (Arroyo de Piedra Formation); (II) Luruaco Anticlinorium (La Popa Formation); (III) SJDB (Toluviejo Formation); (IV) Cicuco Height (Cicuco Limestones). **(c)** Geologic map of the Alta Guajira (after Zuluaga et al., 2009). Roman numbers represent the locations of the stratigraphic sections reported by Silva–Tamayo et al. (2017) for the Siamana Formation: (V) Sillamahana section; (VI) Flor de La Guajira section; (VII) Uitpa Creek section; (VIII) Ekyeps Creek section. **(d)** Geologic map of part of the Western Cordillera of Colombia (after Nivia, 2001) and location of the stratigraphic section (IX) where the Vijes Formation crops out.

bonate textural classification was performed following Dunham (1962) and Embry & Klovan (1971). Facies analyses and environmental interpretations were carried out following Tucker & Wright (2009) and Wilson (2012).

Strontium isotope stratigraphy is an alternative tool to date marine carbonate successions and has been commonly used to complement biostratigraphic analyses (McArthur & Howarth, 2004; McArthur et al., 2012). In this work, we compiled available biostratigraphic information and contrasted it against available and new Sr–isotope chemostratigraphic data to constrain the depositional ages of the reported carbonate successions. The Sr–isotope chemostratigraphic depositional ages were determined by contrasting the $^{87}Sr/^{86}Sr$ values (Table 1) from the studied carbonates against the $^{87}Sr/^{86}Sr$ values of the Cenozoic global seawater reported by McArthur & Howarth (2004) and McArthur et al. (2012) (Figure 7). The chemostratigraphic method relies on the fact that carbonates preserve the isotopic signature of the seawater during their deposition. It also relies on the premise that the Sr isotope composition of the world's oceans is homogeneous in terms of time scales similar to the ocean mixing time, given its residence time of ca. 3 Ma. Because the isotopic signature of the ocean varies through geological time as a result of the imbalances between continental weathering and hydrothermal alteration of the mid–ocean ridges, the evolution of $^{87}Sr/^{86}Sr$ values of marine carbonates has been used to investigate changes in global tectonics (Jacobsen & Kaufman, 1999; Spooner, 1976; Wickman, 1948).

The $^{87}Sr/^{86}Sr$ compositions of carbonates from the Siamana, Arroyo de Piedra, and Toluviejo Formations have been reported elsewhere (Rosero et al., 2014; Salazar–Franco et al., 2016; Silva–Tamayo et al., 2017). Here, we report the $^{87}Sr/^{86}Sr$ compositions of carbonates from the Vijes Formation and La Popa Formation. In all cases, the $^{87}Sr/^{86}Sr$ composition of carbonates was obtained following the methods reported by Rosero et al. (2014) and Silva–Tamayo et al. (2017). Briefly, microdrilled carbonate powders were obtained from polished slabs of carbonate hand samples. Microdrilling was performed to avoid secondary carbonate facies such as telodiagenetic diagenetic cements, carbonate veins, and carbonates derived from weathering. Following Rosero et al. (2014), Salazar–Franco et al. (2016), and Silva–Tamayo et al. (2017), the microdrilled powders were preferentially obtained from the red algal carbonate fraction, excluding those of La Popa Formation, which were obtained from corals.

The microdrilled powders were placed in 15–ml Savillex vials and dissolved in 0.5 M HNO_3. The Sr fraction was separated in Eichron Sr spec columns using 3.5 to 0.05 M HNO_3. The Sr fraction was loaded onto single Re filaments with Ta_2O_5 activator. Mass spectrometric analyses were carried out on an automated VG Sector multi–collector instrument fitted with adjustable 10^{11} ohms faraday collectors and a Daly photomultiplier (Ducea & Saleeby, 1998) at the University of Arizona, Tucson. Typical runs consisted of the acquisition of 100 isotopic ratios. Fifteen analyses of National Institute of Standards and Technology (NIST) standard NBS987 yielded mean ratios of $^{87}Sr/^{86}Sr = 0.710265 \pm 7$ and $^{84}Sr/^{86}Sr = 0.056316 \pm 12$. The Sr isotopic ratios of standards and samples were normalized to the commonly accepted $^{86}Sr/^{88}Sr$ ratio of 0.1194. The estimated analytical (2^{nd}Sdv) uncertainties for samples analyzed in this study were $^{87}Sr/^{86}Sr < 0.0012\%$. Procedural blanks averaged from five determinations were Sr–120 pg.

3. Lithostratigraphy

3.1. Middle to Upper Eocene Carbonates

3.1.1. Arroyo de Piedra Formation

The Arroyo de Piedra Formation occurs along the Luruaco Anticlinorium, the northernmost sector of the San Jacinto deformed belt (SJDB) (Figure 6b; Guzmán, 2007; Guzmán et al., 2004). It was originally described in a stratigraphic section near the municipality of Arroyo de Piedra by Bueno (1970). In this section, the Arroyo de Piedra Formation discordantly overlies the San Cayetano/Arroyo Seco Formation and is discordantly overlain by the Carmen Formation (Figure 5). According to Bueno (1970), the Arroyo de Piedra Formation is ca. 500 m thick, with the thickest sections lying towards the east of the SJDB. It consists of a basal series of thin–bedded siliceous mudstones and gray calcareous mudstones, overlain by a series of lenticular coarse bedded, red algal, biosparitic limestones. Guzmán et al. (2004) suggested that the Arroyo de Piedra Formation is correlative to the Pendales Formation, which also crops out along the Luruaco Anticlinorium (Figure 5). Regionally, the Arroyo de

Table 1. $^{87}Sr/^{86}Sr$ composition of some of the reported carbonate successions (Rosero et al., 2014; Salazar–Franco et al., 2016; Silva–Tamayo et al., 2017; Torres–Lasso, 2014).

Stratigraphic unit	Sample ID	Locality	Carbonate type	$^{87}Sr/^{86}Sr$
La Popa	Boca1(1.35–1.40)	Z–well	Coralline	0.709097
La Popa	Boca1(6.55–6.61)	Z–well	Coralline	0.709106
La Popa	Boca1(9.08–9.02)	Z–well	Coralline	0.709106
La Popa	Boca1(14.33–14.4)	Z–well	Coralline	0.709122
La Popa	LMR–AP–09B	Y–well	Coralline	0.70910
La Popa	LMR–AP–14	Y–well	Coralline	0.70906
La Popa	LMR–MZ–09B	Y–well	Coralline	0.70904
La Popa	LMR–MZ–13	Y–well	Coralline	0.70910
Vijes	VCT–05	Vijes	Rodalgal/Coraline	0.70808
Vijes	VCT–12	Vijes	Rodalgal/Coraline	0.70811
Vijes	VCT–26	Vijes	Rodalgal/Coraline	0.70810
Vijes	VCT–30	Vijes	Rodalgal/Coraline	0.70804
Siamana	540029–5	Parajimaru	Coraline	0.708825
Siamana	540027–5	Parajimaru	Coraline	0.708708
Siamana	540027–1	Parajimaru	Coraline	0.708483
Siamana	540024–1a	Ekyeps Hill	Coraline	0.708502
Siamana	540026–2	Ekyeps Hill	Coraline	0.708368
Siamana	540026–1	Ekyeps Hill	Coraline	0.708324
Siamana	540025–1	Ekyeps Hill	Coraline	0.708348
Siamana	450051	Ekyeps Creek	Rodalgal	0.7086740
Siamana	540050–18	Ekyeps Creek	Rodalgal	0.7086631
Siamana	540050–14	Ekyeps Creek	Rodalgal	0.7086032
Siamana	540050–8	Ekyeps Creek	Rodalgal	0.7086556
Siamana	540050–1	Ekyeps Creek	Rodalgal	0.7086304
Siamana	540051–20	Ekyeps Creek	Rodalgal	0.7086032
Siamana	540051–4	Ekyeps Creek	Rodalgal	0.7085094
Siamana	540052–16	Ekyeps Creek	Coralline	0.7084935
Siamana	540052–13	Ekyeps Creek	Coralline	0.7084850
Siamana	540052–7	Ekyeps Creek	Coralline	0.7084530
Siamana	540052–1	Ekyeps Creek	Coralline	0.7084024
Siamana	540053–11	Ekyeps Creek	Coralline	0.7084000
Siamana	540053–6	Ekyeps Creek	Coralline	0.7083972
Siamana	540053–1	Ekyeps Creek	Coralline	0.7083643
Siamana	540023–4	Uitpa	Rodalgal/Coraline	0.7083850
Siamana	540023–5	Uitpa	Rodalgal/Coraline	0.7083367
Siamana	540023–22	Uitpa	Rodalgal/Coraline	0.7083339
Siamana	540023–23	Uitpa	Rodalgal/Coraline	0.7083119
Siamana	540023–26	Uitpa	Rodalgal/Coraline	0.7081399
Siamana	540023–13d	Uitpa	Rodalgal/Coraline	0.7081267
Siamana	540023–18a	Uitpa	Rodalgal/Coraline	0.7081284
Siamana	540023–19	Uitpa	Rodalgal/Coraline	0.708142
Siamana	540025–1	Uitpa	Rodalgal/Coraline	0.7081475
Siamana	540023–2	Uitpa	Rodalgal/Coraline	0.708131

Table 1. $^{87}Sr/^{86}Sr$ composition of some of the reported carbonate successions (Rosero et al., 2014; Salazar–Franco et al., 2016; Silva–Tamayo et al., 2017; Torres–Lasso, 2014) (*continued*).

Stratigraphic unit	Sample ID	Locality	Carbonate type	$^{87}Sr/^{86}Sr$
Siamana	540023–1	Uitpa	Rodalgal/Coraline	0.7081855
Siamana	540054–21	Sillamahana	Rodalgal/Coraline	0.70354
Siamana	540054–19	Sillamahana	Rodalgal/Coraline	0.7082140
Siamana	540054–14	Sillamahana	Rodalgal/Coraline	0.7081452
Siamana	540054–10	Sillamahana	Rodalgal/Coraline	0.7081245
Siamana	540054–6	Sillamahana	Rodalgal/Coraline	0.7080420
Siamana	540054–3	Sillamahana	Rodalgal/Coraline	0.7080300
Siamana	540054–1	Sillamahana	Rodalgal/Coraline	0.7080300
Siamana	540030–1	Flor Guajira	Rodalgal/Coraline	0.708854
Siamana	540030–2	Flor de La Guajira	Rodalgal/Coraline	0.708385
Siamana	540030–3	Flor de La Guajira	Rodalgal/Coraline	0.708158
Siamana	540030–4	Flor de La Guajira	Rodalgal/Coraline	0.7080635
Siamana	540030–5	Flor de La Guajira	Rodalgal/Coraline	0.7080317
Macarao	360150–1	Flor de La Guajira	Rodalgal	0.707911
Macarao	360150–5	Flor de La Guajira	Rodalgal	0.707843
Macarao	360150–13	Flor de La Guajira	Rodalgal	0.707867
Macarao	360153–26	Flor de La Guajira	Rodalgal	0.7078023
Toluviejo	P8 279.57	P8–well	Rodalgal	0.70762
Toluviejo	P8 274.99	P8–well	Rodalgal	0.70760
Toluviejo	P8 264.19	P8–well	Rodalgal	0.70757
Toluviejo	P8 220.13	P8–well	Rodalgal	0.70742
Toluviejo	P8 204.59	P8–well	Rodalgal	0.70744
Toluviejo	P8 203.85	P8–well	Rodalgal	0.70750
Toluviejo	P8 198.49	P8–well	Rodalgal	0.70746
Toluviejo	P8 193.06	P8–well	Rodalgal	0.70735
Toluviejo	P8 192.49	P8–well	Rodalgal	0.70744
Arroyo de Piedra	PP–01	Arroyo de Piedra	Rodalgal	0.707729
Arroyo de Piedra	PP–04	Arroyo de Piedra	Rodalgal	0.707638
Arroyo de Piedra	PP–08	Arroyo de Piedra	Rodalgal	0.707776
Arroyo de Piedra	PP–11	Arroyo de Piedra	Rodalgal	0.707762
Arroyo de Piedra	PP–13	Arroyo de Piedra	Rodalgal	0.707729
Arroyo de Piedra	PP–16	Arroyo de Piedra	Rodalgal	0.707751
Arroyo de Piedra	AP–01	Arroyo de Piedra	Rodalgal	0.707743
Arroyo de Piedra	AP–02	Arroyo de Piedra	Rodalgal	0.707739
Arroyo de Piedra	AP–04	Arroyo de Piedra	Rodalgal	0.707734
Arroyo de Piedra	AP–05	Arroyo de Piedra	Rodalgal	0.707734
Arroyo de Piedra	AP–09	Arroyo de Piedra	Rodalgal	0.707763
Arroyo de Piedra	AP–10	Arroyo de Piedra	Rodalgal	0.707676
Arroyo de Piedra	AP–15	Arroyo de Piedra	Rodalgal	0.707286
Arroyo de Piedra	AP–19	Arroyo de Piedra	Rodalgal	0.707717
Arroyo de Piedra	AP–22	Arroyo de Piedra	Rodalgal	0.707718
Arroyo de Piedra	7701’6”	X–well	Rodalgal	0.707707
Arroyo de Piedra	7697’4”	X–well	Rodalgal	0.707772

Table 1. $^{87}Sr/^{86}Sr$ composition of some of the reported carbonate successions (Rosero et al., 2014; Salazar–Franco et al., 2016; Silva–Tamayo et al., 2017; Torres–Lasso, 2014) (*continued*).

Stratigraphic unit	Sample ID	Locality	Carbonate type	$^{87}Sr/^{86}Sr$
Arroyo de Piedra	7695'	X–well	Rodalgal	0.707764
Arroyo de Piedra	7693'3"	X–well	Rodalgal	0.707834
Arroyo de Piedra	7688'5"	X–well	Rodalgal	0.707717
Arroyo de Piedra	7682'3"	X–well	Rodalgal	0.707990
Arroyo de Piedra	7680'6"	X–well	Rodalgal	0.707768
Arroyo de Piedra	7678'10"	X–well	Rodalgal	0.707749
Arroyo de Piedra	7675'3"	X–well	Rodalgal	0.707699

Piedra Formation is correlated with the Toluviejo, San Jacinto, Maco, Chengue, and Tampa Formations (Figure 5). Although no paleontological data have been published, DUQUE–CARO in Guzmán et al. (2004) suggests that the Arroyo de Piedra Formation was deposited during the middle Eocene (Lutetian) to early Oligocene (earliest Rupelian).

Recently, Salazar–Franco et al. (2016) studied the carbonates of the Arroyo de Piedra Formation near the type locality and in cores from one stratigraphic well (Well–X). The lower part of the Arroyo de Piedra Formation displays thin–to–medium bedded aggradational gray siltstones, with parallel lamination and abundant wood fragments (Figure 8a). Occasionally, thin–to–medium lenticular beds of packstones and grainstones with fragments of red algae and clay intraclasts are present. LBF as well as traces of bryozoans, corals, and echinoderm fragments can also be found. Bioclastic limestones, mixed carbonate–siliciclastic (grainstones, packstones, and rudstones with intraclasts) and, to a lesser proportion, fine–grain siliciclastic sedimentites overlay the abovementioned strata (Figure 8a). The bioclastic calcareous segments are composed of massive rhodolith rudstones, distributed in thick layers, with tabular and irregular geometries. These strata are overlaid with packstones, rudstones, and grainstones with abundant intraclasts with a clay to silt composition, arranged in middle layers with cross–stratification and lenticular and channel–shaped geometries. Calcareous red algae, LBF (*Orbitoides*, *Discocyclina*, *Nummulites*), other benthic foraminifera (Miliolids and Fusulinids), and planktonic foraminifera constitute the main allochemical components of these uppermost carbonate packages (Figure 8b–d).

Salazar–Franco et al. (2016) reported $^{87}Sr/^{86}Sr$ values between 0.707714–0.707771 for carbonates from the lower part of the Arroyo de Piedra Formation (Figure 7). According to these authors, such values correspond to 41–35 Ma, suggesting a middle to late Eocene (Lutetian – Priabonian) depositional age. For the middle part of the Arroyo de Piedra Formation, the same authors reported $^{87}Sr/^{86}Sr$ values between 0.707638–0.707776, which corresponds to 39–33.9 Ma, and suggested a middle to late Eocene (Bartonian – Priabonian) depositional age. The $^{87}Sr/^{86}Sr$ values between 0.707699–0.707834 (35–33 Ma) displayed by the upper carbonates were used by Salazar–Franco et al. (2016) to suggest a late Eocene (Priabonian) – early Oligocene (Rupelian) depositional age for the uppermost carbonates of the Arroyo de Piedra Formation. The Sr–isotope chemostratigraphic ages reported by Salazar–Franco et al. (2016) not only overlap the foraminifera biostratigraphic ages (Lutetian – Rupelian) ages reported by DUQUE–CARO in Guzmán et al. (2004) but also provide clues regarding the temporal evolution of the Arroyo de Piedra carbonates.

3.1.2. Macarao Formation

The Macarao Formation crops out along the Cocinetas Sub–basin, Alta Guajira Basin, and La Guajira Department, Colombia (Figure 6). It was initially defined by Renz (1960) and redefined by Rollins (1960) and Thomas (1972). The type section of the Macarao Formation is located near the "Flor de La Guajira" locality in the northeastern most part of La Guajira Department (Figure 6c; Rollins, 1960; Thomas, 1972). At this locality, the Macarao Formation is ca. 250 m thick and unconformably overlies the deformed Upper Cretaceous marine sedimentary successions of the Cocinas Range (Figure 5). Oligocene – Miocene marine carbonates from the Siamana Formation unconformably overlay the Macarao Formation (Rollins, 1960; Thomas, 1972). In its type section, the Macarao Formation consists of a series of glauconitic micaceous sandstones interbedded with thick massive fossiliferous mudstones and limestones (Rollins, 1960). It has been correlated with the Nazareth Formation of the Alta Guajira Basin and La Sierra Formation from the serranía de Perijá (Renz, 1960).

For this chapter, we studied the Macarao Formation near to its type section along the Cocinetas Sub–basin, Alta Guajira Basin, Colombia (Figure 6a, 6c). Although Rollins (1960) suggested that the Macarao Formation is ca. 250 m thick in its type section, in the new studied stratigraphic section, the Macarao Formation is only ca. 150 m thick (Figure 9a). The difference in thickness is due to the highly deformed nature of this stratigraphic unit in its type locality. In the new locality, the Macarao Formation consists of a series of tabular–aggradational rhodolithic grainstones, interbedded with a series of

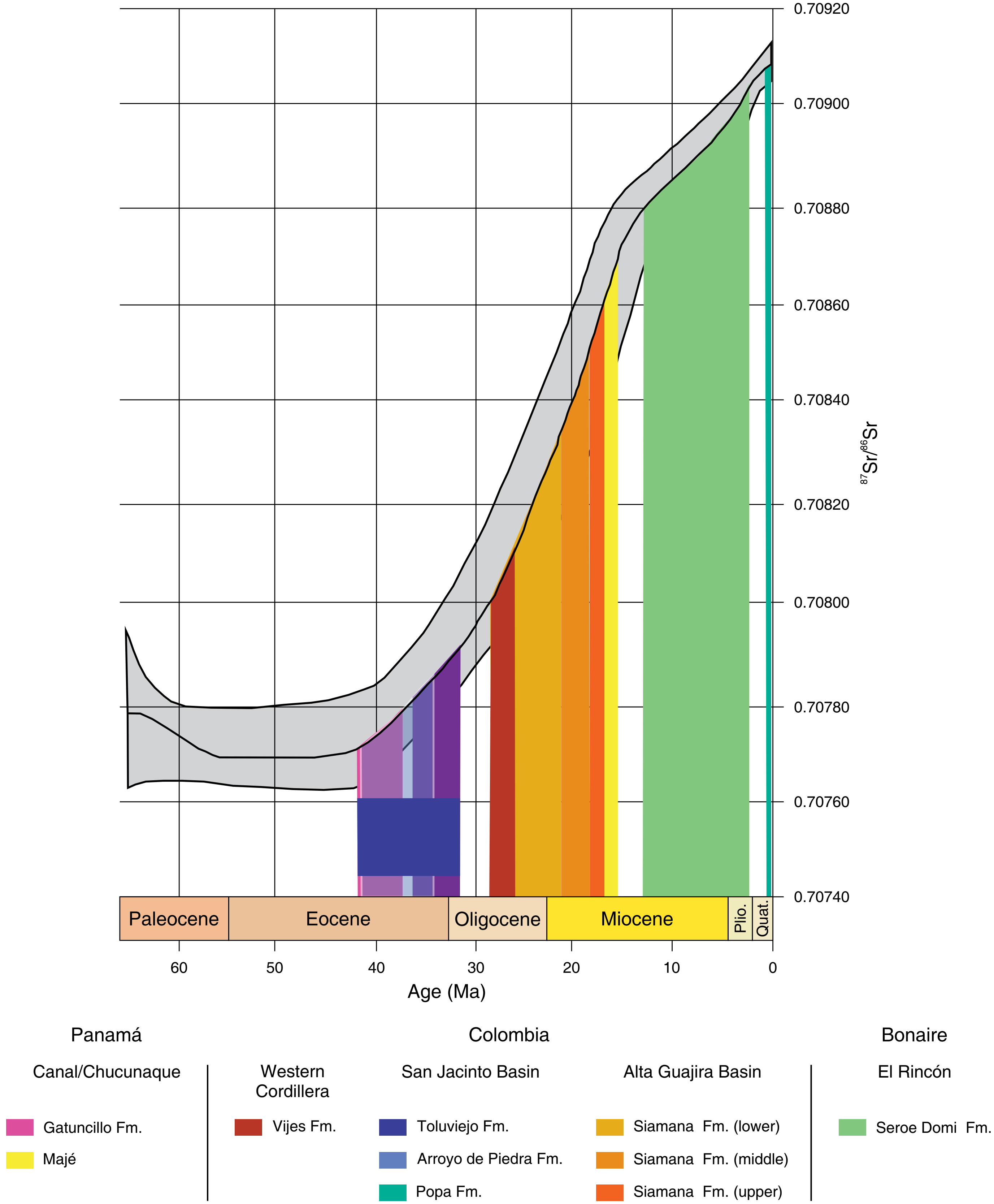

Figure 7. Evolution of the $^{87}Sr/^{86}Sr$ composition of the seawater and range of compositions of some of the reported carbonate successions. The Sr chemostratigraphic ages of carbonates were determined based on the correspondence of their $^{87}Sr/^{86}Sr$ compositions (see Table 1) and that of the seawater.

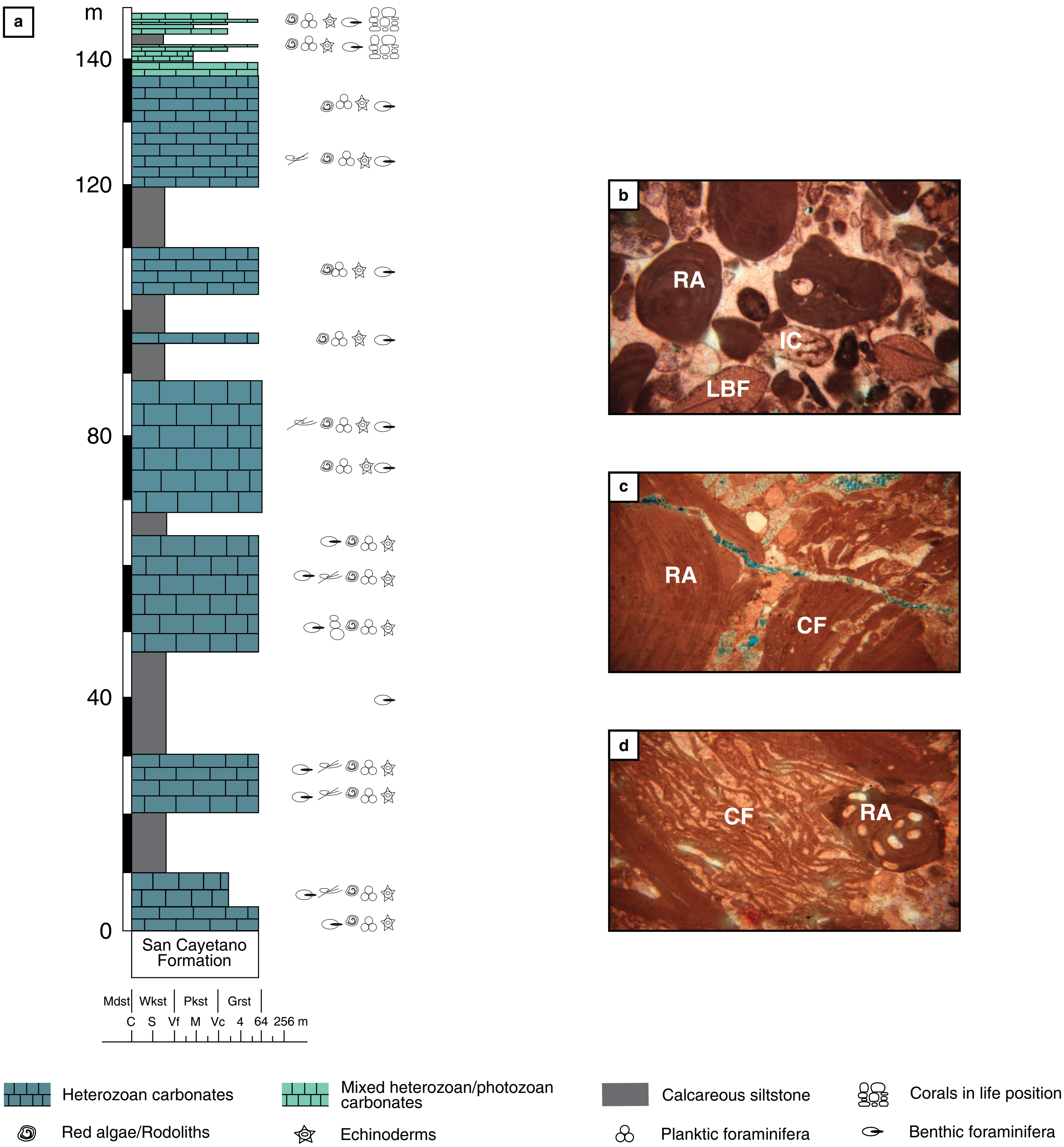

Figure 8. (a) Generalized lithostratigraphic column of the Arroyo de Piedra Formation along the Luruaco Anticlinorium. **(b)** Packstones with reworked red algal fragments (RA), intraclasts (IC), and larger benthic foraminifera (LBF). **(c)** Grainstone with fragments of corals (CF) and red algae (RA). **(d)** Grainstone with fragments of corals (CF) and red algae (RA).

quartz rich glauconitic sandstones (Figure 9a). In addition to coralline algae, the most common allochemicals of the grainstones are LBF (mainly *Nummulites* and lepidocyclinids), mollusks, bryozoans, and echinoderms. Mollusk and foraminifera are found unfragmented, while bryozoans, echinoderms, and rhodoliths are often fragmented (Figure 9b–d).

Carbonates from the Macarao Formation display $^{87}Sr/^{86}Sr$ values between 0.7078023 and 0.707911 (Table 1). These

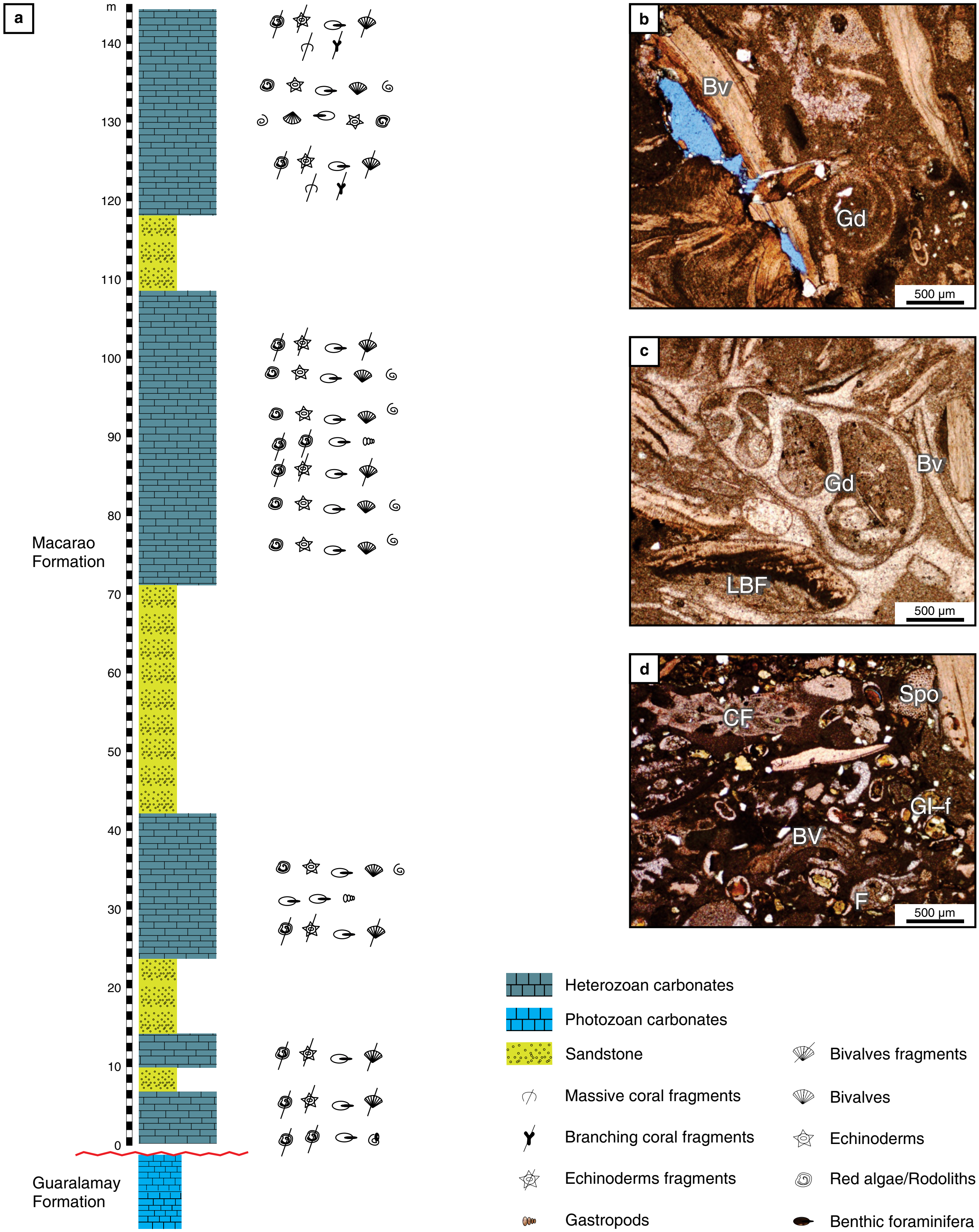

Figure 9. **(a)** Generalized lithostratigraphic column of the Macarao Formation. **(b)** Photomicrograph of grainstone with gastropods (Gd) and bivalves (Bv). **(c)** Photomicrograph of a grainstone with gastropods (Gd), bivalves (Bv), and larger benthic foraminifera (LBF). **(d)** Photomicrograph of a packstone with coral fragments (CF), sponge fragments (Spo), bivalves (BV), planktic foraminifera (F), and glauconite cement replacing foraminifera (Gl–f).

values correspond to 36–32 Ma and suggest a late Eocene (Priabonian) depositional age. These ages partially overlap the foraminifera biostratigrahic ages suggested by (Rollins, 1960; Thomas 1972).

3.1.3. Toluviejo Formation

The Toluviejo Formation crops out along the central part of the SJDB. It was originally named "Series de Toluviejo" (Guzmán et al., 2004). Kassem et al. (1967) and Duque–Caro (1968) proposed the formal name of the Toluviejo Formation for this stratigraphic unit. Although no official type section has been proposed for the Toluviejo Formation, the most accepted type locality is near the Toluviejo municipality, Sucre Department, Colombia. According to Guzmán et al. (2004), the Toluviejo Formation unconformably overlays the late Paleocene – early Eocene San Cayetano Formation and is unconformably overlain by the Oligocene Carmen Formation. According to Guzmán et al. (2004), in its type section, the Toluviejo Formation mainly consists of a series of brown limestones with abundant lepidocycline macroforaminifers, *Nummulites*, red algal rhodoliths, oncoliths, and fragments of echinoderms and mollusks. It also displays fine–to–medium–grained lithic sandstones and coarse–grained carbonate–rich sandstones with abundant glauconite, marls, gray mudstones, and fine–to–medium–grained sandstones. Previous analyses of planktonic foraminifera (Bermúdez et al., 2009; Duque–Caro, 1975; Guzmán et al., 2004), palynology (Alfonso et al., 2009; Bermúdez et al., 2009), LBF (Alfonso et al., 2009), and calcareous nannofossils (Bermúdez et al., 2009) suggested a middle to late Eocene age (Lutetian – Priabonian) for the Toluviejo Formation. Additionally, DUQUE–CARO in Guzmán et al. (2004) correlates it with the Arroyo de Piedra and Pendales Formations of the Luruaco Anticlinorium and the Chengue, Maco, San Jacinto, and Tampa Formations from the central and southern part of the SJDB.

Near the type locality, at Porvenir Hill (Figures 6b, 10b), the Empresa Colombiana de Petróleos S.A. (Ecopetrol) obtained a detailed description of the sedimentological characteristics from the Toluviejo Formation (Ortiz et al., 1998). In this section, the lowermost part of the Toluviejo Formation displays a series of calcareous sandy siltstones, composed of very fine sand–sized quartz grains, within a calcareous matrix. Locally, concentrations of LBF (Orbitoidacea, *Discocycline*, and *Nummulites*) are observed, as well as *Thallasinoides* burrows and undifferentiated bioturbation (Figure 10). Higher in the stratigraphy, red algae rhodolith packstones, displaying sponges, LBF (Orbitoidacea and *Discocyclina*), and benthic foraminifera (Nodosariacea, Buliminacea) occur, as well as fragments of corals, pelecypods, and ostracods. A thin–bedded boundstone layer of sponges and *Acropora* coral fragments has been found interbedded with a rhodolithic packstone. The upper part of the Toluviejo Formation displays fine–grained, mud–supported, lithic arkose, with the presence of pelecypods shells, echinoderm spicules, and LBF (*Nummulites*).

In a northern stratigraphic section, Bermúdez et al. (2009) and Rosero et al. (2014) studied the Toluviejo Formation in the core ANH P–8 well (Figures 6b, 10a). In this core, the Toluviejo Formation discordantly overlies the San Cayetano/Arroyo Seco Formation (Figure 10a). It consists of thick layers of interbedded sandstones and aggradational fossiliferous wackestones and packstones. Rhodoliths and millimetric–to–centimetric benthic foraminifera (mainly *Nummulites* and lepidocyclinids) constitute the main allochems of these carbonates. The wackestones also display decimeter oncoids, mollusks, and echinoderms as subordinate allochems (Figure 10c–e).

Rosero et al. (2014) used $^{87}Sr/^{86}Sr$ chemostratigraphy in to determine the depositional age of the Toluviejo Formation. They reported $^{87}Sr/^{86}Sr$ values between 0.707444–0.707598 for carbonates from the AHN P–8 well. These values fall below those displayed by global Cenozoic carbonates and therefore below the accepted values for the Cenozoic seawater (Figure 7). According to Rosero et al. (2014), the low $^{87}Sr/^{86}Sr$ values displayed by carbonates from the Toluviejo Formation do not reflect the seawater values and therefore cannot be used to infer the depositional age of the Toluviejo Formation in the P–8 well. Foraminifera and calcareous nannofossil assemblages reported for the P–8 well suggest a late Eocene (Priabonian) to early Oligocene (Rupelian) depositional age (Bermúdez et al., 2009). Salazar–Franco et al. (2016) used these depositional ages, as well as lithology and carbon and oxygen isotopes, to correlate the upper Arroyo de Piedra Formation and the Toluviejo Formation (P–8 well).

3.2. Late Oligocene to Early Miocene Carbonates

3.2.1. Ciénaga de Oro Formation

The Ciénaga de Oro Formation was first referred to in internal reports of the company Intercol (Guzmán et al., 2004). It crops out along the central and southern part of the SJDB of the San Jacinto Basin, and it is also found in the subsurface along the Lower Magdalena Valley Basin along the San Jorge and Plato Sub–basins. The Ciénaga de Oro Formation mainly consists of deltaic siliciclastic successions, which display fining–upward packages of fine to coarse–grained sandstones interbedded with fossiliferous siltstones. Based on both palynology (Bermúdez et al., 2009; Dueñas, 1977, 1986) and planktonic foraminiferal data (Bermúdez et al., 2009), an Oligocene – middle Miocene depositional age has been proposed for the Ciénaga de Oro Formation. This formation has been correlated with siltstone–

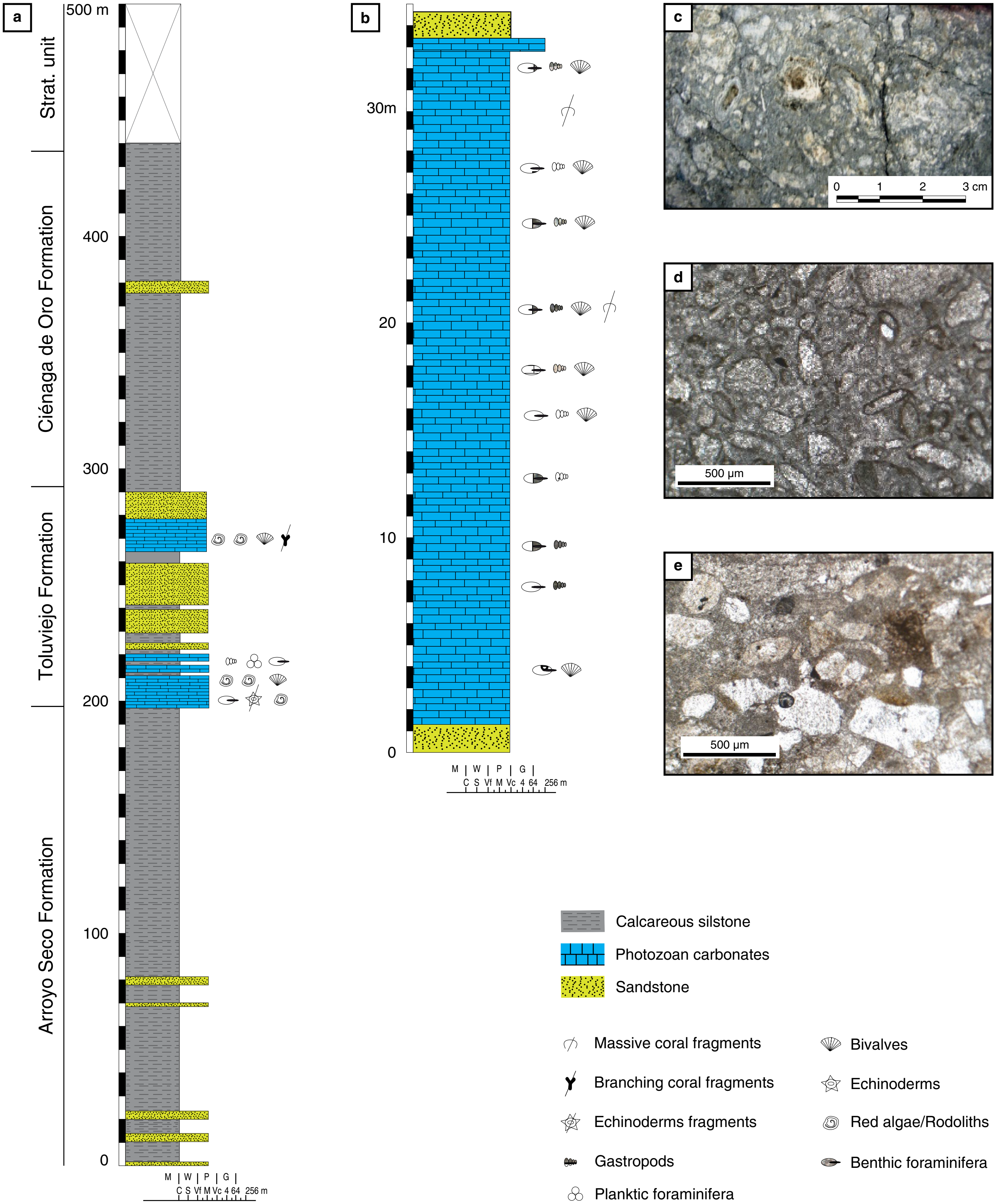

Figure 10. Generalized lithostratigraphic column of the Toluviejo Formation. **(a)** Slim–hole P–8 from the Agencia Nacional de Hidrocarburos (After Bermúdez et al., 2009). **(b)** Porvenir Hill section stratigraphic column (After Ortiz et al., 1998). **(c)** Hand sample of rhodolithic limestone. **(d)** Photomicrograph of coral fragment. **(e)** Photomicrograph of wackestone displaying echinoderm fragments and quartz sand.

dominated successions from the Carmen and Floral Formations from the central and northern parts of the Lower Magdalena Valley Basin (Bermúdez et al., 2009).

In the Plato Sub–basin, the Ciénaga de Oro Formation also displays subordinate carbonate packages, which occur in the subsurface (Figure 5; Reyes–Harker et al., 2000). Some of those packages have been reported in El Difícil and Cicuco gas oil fields (Ortiz & Niño, 1999). Swolf (1946) originally reported the sedimentological characteristics of the Ciénaga de Oro Formation limestones (Cicuco Limestones). Ortiz & Niño (1999) analyzed cores from thirteen wells in the Cicuco and Boquete fields, drilled between the Brazo de Mompós and Brazo de Loba in the Lower Magdalena Valley (Figure 6b). The authors found that in all wells, the Cicuco Limestones conformably overlays a series of basal conglomeratic sandstones, which display fragments of pelecypods and gastropods, as well as abundant uniserial benthic foraminifera (Figure 11). The basal conglomeratic sandstones are overlain by sandy limestones, which grade to pure limestones towards the top. These limestones mainly display LBF (*Sorites*) and mollusk shell fragments. Higher in the stratigraphy, calcareous sandstones are present, which are rich in shell fragments from gastropods and pelecypods. Such calcareous sandstones grade to sandy limestones and wackestones, the main allochemical components of which are benthic foraminifera, echinoderms, corals, and red algae (*Lithophyllum*). A series of coral and red algal packstones/wackestones, characterized by abundant skeletal fragments consisting mainly of coral heads and branching corals (*Porites*), with variable amounts of large echinoderm spines, pelecypod shell fragments, benthic foraminifera, and rhodoliths, occur higher in the stratigraphic section. Boundstones, rudstones, and floatstones, characterized by abundant coral debris (*Porites, Diploastrea*, *Montastrea*, *Siderastrea*), LBF (*Operculinoides*, *Heterostegina*, *Lepidocyclina*), mollusk shell fragments, and red algae (*Mesophyllum*, *Lithophyllum*, and rhodoliths), also occur in the uppermost part of the Cicuco Limestones (Figure 11). Overlying the limestone in some wells are found terrigenous and bioclast rich grainstones and calcareous sandstone (Ortiz & Niño, 1999).

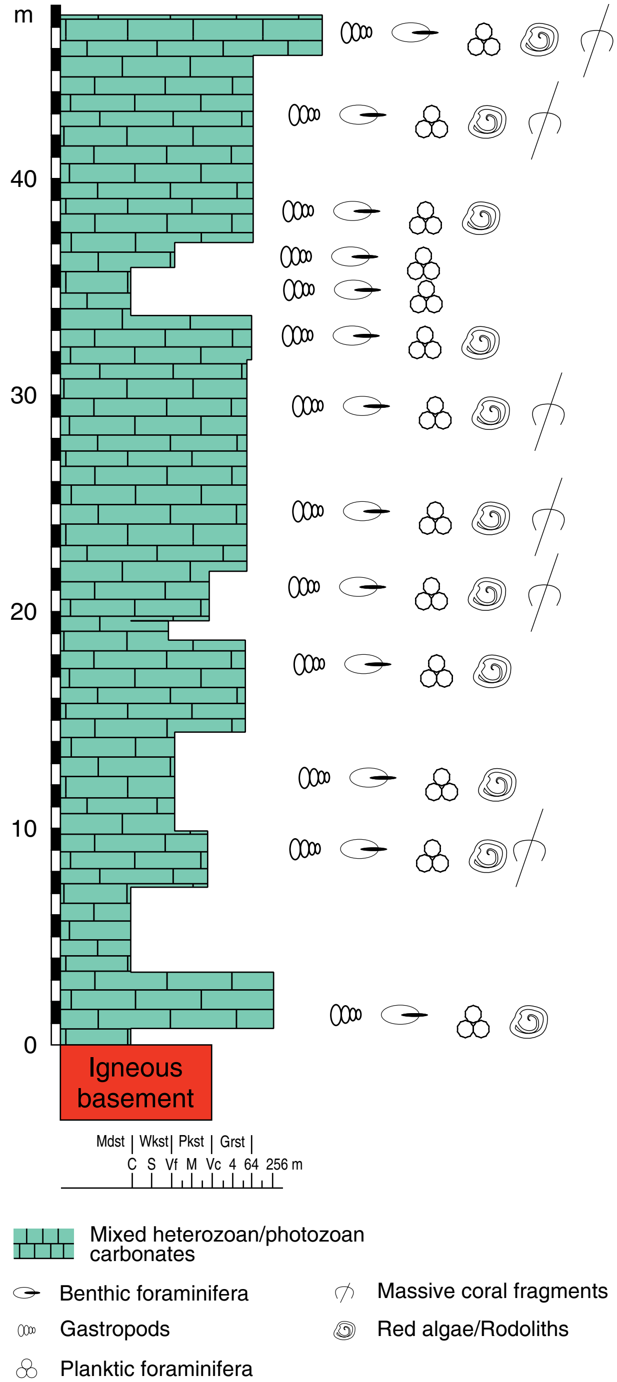

Figure 11. Generalized lithostratigraphic column of the Cicuco Limestones (Ciénaga de Oro Formation) (Ortiz & Niño, 1999).

3.2.2. Siamana Formation

The Siamana Formation was originally defined by Renz (1960). It crops out around the Macuira and Jarara Ranges and to the north of the Cosinas Range, along the Cocinetas Sub–basin of the Alta Guajira Basin, La Guajira Department, Colombia (Figure 6c). The type section of the Siamana Formation is located near the Sillamahana locality. According to Renz (1960), the Siamana Formation consists of a basal series of marly polymictic conglomerates followed by a series of fossiliferous sandy limestones interspersed with mudstones and shales, with abundant bivalves and gastropods (Rollins, 1960). Locally, thin layers of calcareous and fine–grained clayey sandstones are present. Higher in the section, the development of coral reef limestones is common (Rollins, 1960).

Silva–Tamayo et al. (2017) studied the Siamana Formation using surface stratigraphic sections along the Cocinetas Sub–basin, Alta Guajira Basin, northern Colombia (Figure

6a). According to these authors, the undeformed Siamana Formation discordantly overlies the deformed Macarao Formation, as well as the pre–Cenozoic crystalline basement of the Cosinetas Sub–basin. The basal part of the Siamana Formation (Sillamahana and Flor de La Guajira sections; Figure 12a–c) consists of mixed carbonate siliciclastic successions, in which polymictic conglomerates are interbedded with restricted framestones, rudstones, grainstones, and wackestones. The framestones, which are mostly composed of massive corals, are also found unconformably capping the deformed Macarao Formation (Figure 12b, 12d). Massive corals, echinoderms, and calcareous algae constitute the main allochemical components of rudstones, grainstones, and wackestones. The basal mixed carbonate siliciclastic succession is overlain by a series of packstone, grainstones, rudstones, and framestones. The framestones mainly consist of massive and ramified corals (Figure 12d). Ramified corals constitute the predominant component of the rudstones. Instead, coral fragments, brachiopods, echinoderms, and bivalves are the main allochemical components of packstones and grainstones, which also contain LBF (*Nummulites*) and benthic foraminifera (Miliolids, Fusulinids) (Figure 12e, 12f). While the packstones and grainstones are the most predominant, they are not laterally continuous and vary laterally to restricted framestones and rudstones. The middle part of the Siamana Formation (Uitpa stratigraphic section, Figure 13) displays a basal series of boundstones, bafflestones, and framestones, characterized by a highly diverse coral assemblage; i.e., ramose, platy, and massive corals (Figure 13b–e). These facies extend laterally for several kilometers and display predominantly aggradational stacking patterns that change laterally (locally) to fining–upward grainstones and packstones, consisting of fragments of corals, mollusks, echinoderms, bivalves, and foraminifera. The uppermost part of the Siamana Formation displays a series of laterally continuous (kilometrical) aggradational strata, mainly composed of centimeter–to–decimeter rhodalgal biostromes (Ekyeps Creek stratigraphic section, Figure 14a). Echinoderms and foraminifera constitute subordinate allochems of these biostromes. These coralline algae successions are finally overlain by a series of fining upward cycles of grainstones to packstones constituted predominantly by coralline algae fragments and foraminifera (Figure 14b–e).

Carbonates from the lower part of Siamana Formation display $^{87}Sr/^{86}Sr$ values between 0.708030 and 0.708385 (Figure 7), suggesting a late Oligocene (Chattian) – early Miocene (Aquitanian) depositional age (28–22 Ma). $^{87}Sr/^{86}Sr$ values between 0.708348 and 0.708485 are displayed by carbonates from the middle part of the Siamana Formation (Figure 7), suggesting a depositional age of early Miocene (Aquitanian – Burdigalian), between 21 and 18 Ma (Silva–Tamayo et al., 2017). Carbonates from the upper part of the Siamana Formation display $^{87}Sr/^{86}Sr$ values between 0.708502 and 0.708674, suggesting a depositional age of early to middle Miocene (Burdigalian – Langhian), between 18 and 15 Ma (Figure 7).

3.2.3. Vijes Formation

The Vijes Formation crops out along the eastern flank of the Western Cordillera of Colombia and west of the Cauca–Patía Basin (Dueñas et al., 2000). Its type section is located near the town of Vijes, Valle del Cauca Department, southwestern Colombia (Figure 6d). Dueñas et al. (2000) reported the first lithostratigraphic information on the Vijes Formation from stratigraphic cores. According to these authors, the Vijes Formation unconformably overlies the volcanic basement of the Western Cordillera of Colombia. The lower part of the Vijes Formation displays polymictic conglomerates overlain by a series of coral and red algae–rich limestones. The middle part of the Vijes Formation displays, in turn, alternating mudstones and fine–grained sandstones. The upper part of the formation mostly displays quartz sandstones. Dueñas et al. (2000) used the occurrence of the foraminiferal biozones P18–P21 to suggest an Oligocene (Rupelian – Chattian) depositional age for the Vijes Formation.

In this chapter, we further study the Vijes Formation in a surface stratigraphic section (Figure 6d). In this section, the Vijes Formation is approximately 130 m thick and displays a basal polymictic conglomerate overlain by a series of alternating coarsening–upward, and fining–upward packages of wackestones, packstones, and grainstones (Figure 15a). These sedimentary packages display abundant LBF, fragments of bivalves, echinoderms, gastropods, and occasionally bryozoans, calcareous red algae fragments, and oncoliths. These carbonate packages also display variable amounts of fine–grained quartz sand. Higher in the stratigraphy, the sedimentary succession displays a coarsening–upward character, and the sedimentary packages become thicker and more aggradational. The wackestones display abundant coarse conglomeratic sand and angular quartz fragments, as well as foraminifera, algae, mollusks, and oncoliths. The grainstones display fragments of algae, gastropods, and bivalves. A new fining–upward set of strata displaying grainstones, packstones, and wackestones is observed higher in the stratigraphy. Carbonates from this new set display fragments of algae, foraminifera, and mollusk, as well as abundant quartz. The upper part of the sedimentary succession displays aggradational packages of packstones and wackestones. Algae, gastropods, bivalves, and echinoderms are the main allochemical components. These aggradational carbonate packages are overlain by a series of massive sandstones with low fossil content. The uppermost part of the sedimentary succession displays a set of coarsening upward sandstones, which display fragments of algae, mollusks, and foraminifera. Some grainstones with abundant quartz sand and fragments of algae, foraminifera, and mollusks also occur in this part of the sedimentary succession (Figure 15b–e).

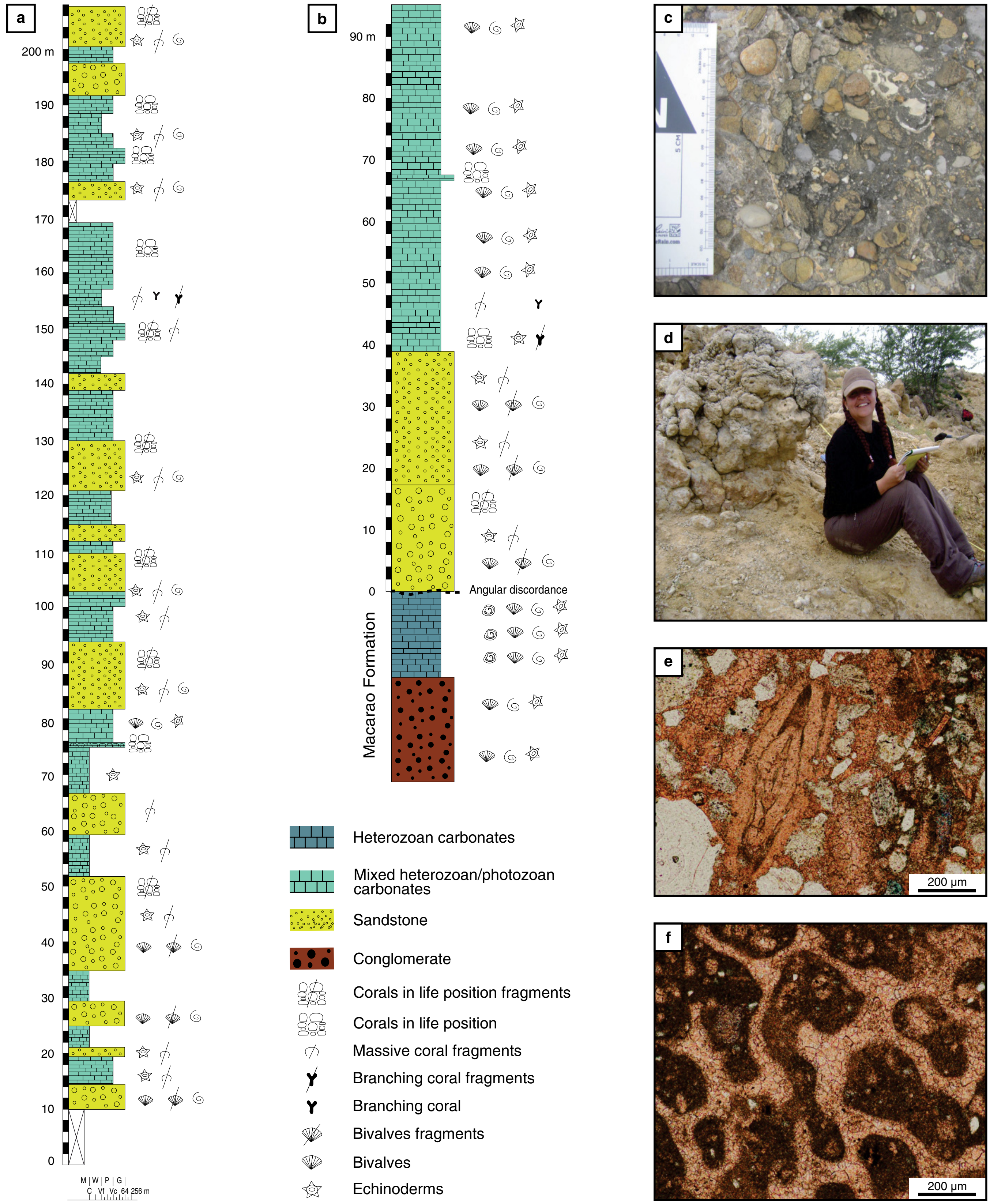

Figure 12. Generalized lithostratigraphic column of the lowermost Siamana Formation (Silva–Tamayo et al., 2017). **(a)** Sillamahana stratigraphic section. **(b)** Flor de La Guajira stratigraphic section. **(c)** Basal conglomerate in the Sillamahana section. **(d)** Framestone from the lowermost part of the Flor de La Guajira stratigraphic section. **(e)** Photomicrograph of a packstone displaying larger benthic foraminifera (LBF) and quartz sand (Q). **(f)** Photomicrograph of a coral fragment.

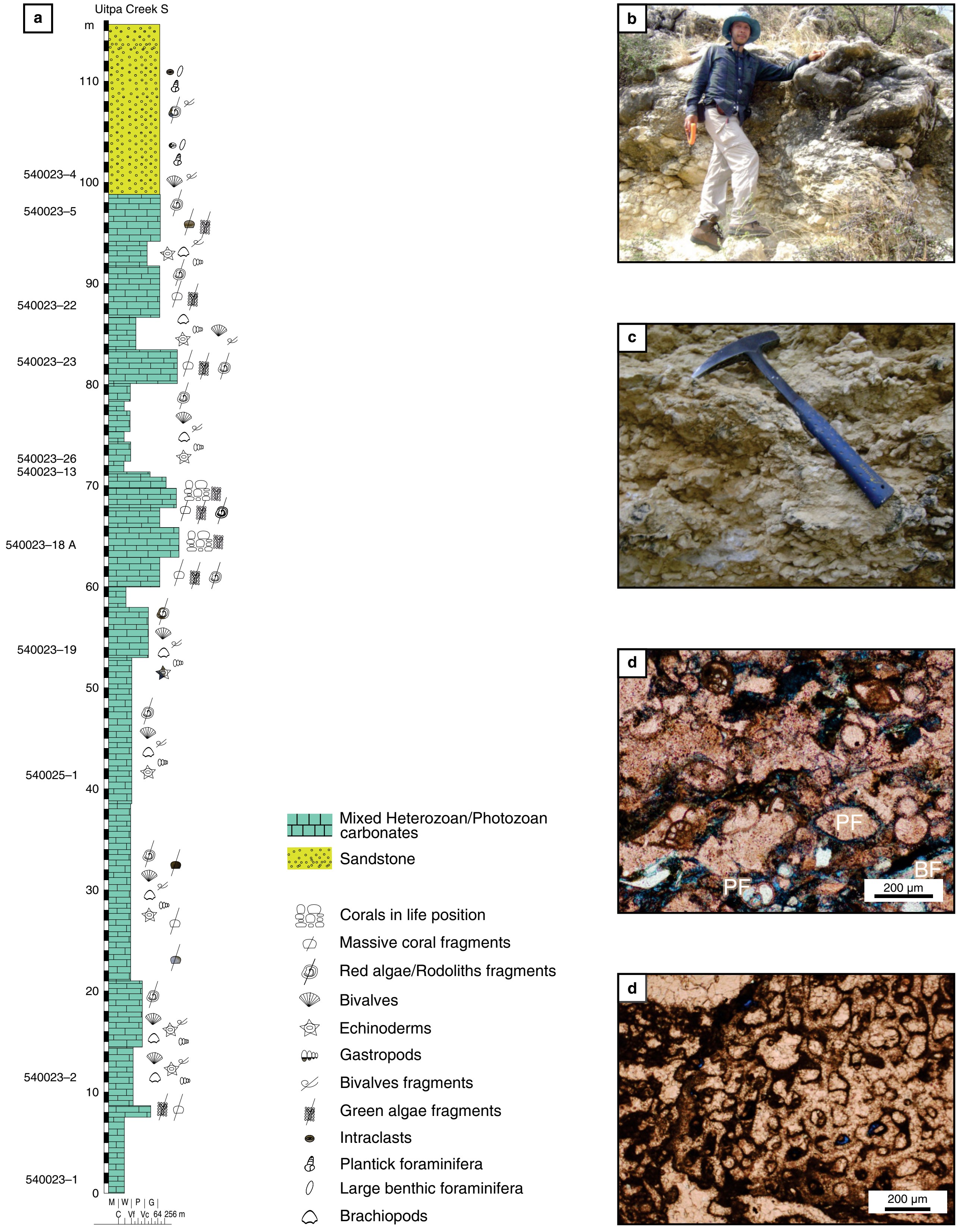

Figure 13. (a) Generalized lithostratigraphic column of the middle part of the Siamana Formation in the Uitpa Creek stratigraphic section (Silva–Tamayo et al., 2017). **(b)** Framestones from the upper part of the stratigraphic section. **(c)** Rudstone from the lowermost part of the stratigraphic section. **(d)** Photomicrograph of a packstone from the middle part of the stratigraphic section displaying planktic foraminifera (PF) and bivalve fragments (BF). **(e)** Photomicrograph of a coral fragment of framestone from the uppermost part of the stratigraphic section.

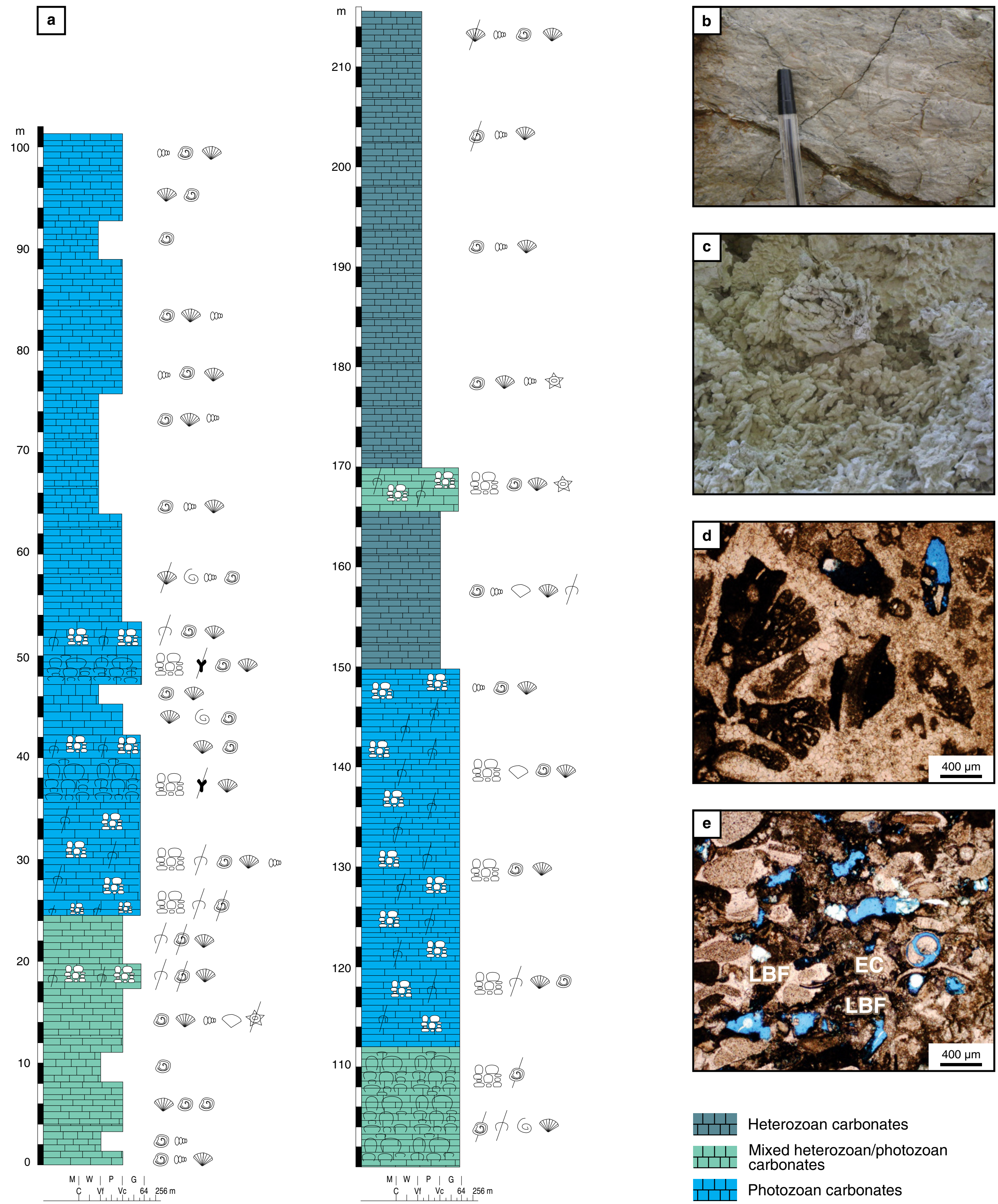

Figure 14. (a) Generalized lithostratigraphic column from the upper part of the Siamana Formation of the Ekyeps Creek stratigraphic sections (Silva–Tamayo et al., 2017). **(b)** Large benthic foraminifera grainstone from the uppermost part of the Siamana Formation. **(c)** Framestone from the lower part of the Ekyeps Creek stratigraphic section. **(d)** Photomicrograph of coral fragment from the lower part of the stratigraphic section. **(e)** Photomicrograph of grainstone from the middle part of the stratigraphic section. (EC) Echinoderm; (LBF) larger benthic foraminifera.

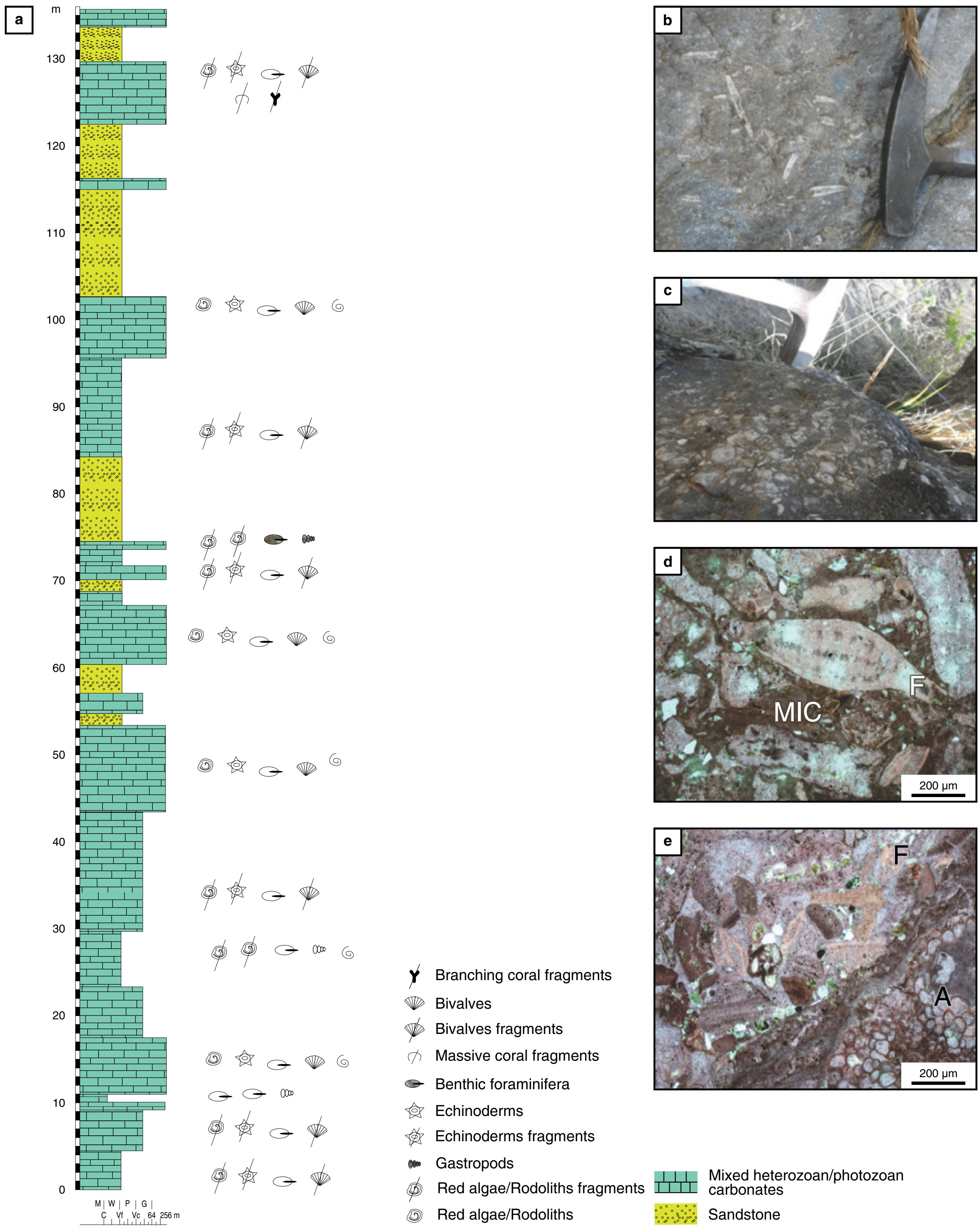

Figure 15. (a) Generalized lithostratigraphic column of the Vijes Formation (Torres–Lasso, 2014). **(b)** Grainstone displaying rhodolith and gastropods. **(c)** Rhodolith from the lower part of the Vijes Formation. **(d)** Photomicrography of a grainstone from the upper part of the Vijes formation displaying benthic foraminifera (F) and micritic cement (MIC). **(e)** Photomicrograph of grainstone from the lowermost part of the Vijes Formation displaying green algal fragments (A) and benthic foraminifera (F).

Carbonates from the Vijes Formation display $^{87}Sr/^{86}Sr$ values between 0.708035 and 0.708111 (Figure 7). These values suggest a late Oligocene (Chattian) depositional age, between 26–28 Ma. The Chattian age partially overlaps those proposed for the Vijes Formation based on palynomorphs and foraminifera biostratigraphy (Dueñas et al., 2000).

3.3. Middle to Late Miocene Carbonates

3.3.1. San Andrés Formation

The middle – late Miocene San Andrés Formation was first described by Hubach (1956). It crops out in the center of the San Andrés Island, Colombia, along the Los Cayos Basin of the Lower Nicaragua Rise (Figure 6a). No type section has been proposed for the San Andres Formation. The available lithostratigraphic information comes from well cores from the Servicio Geológico Colombiano (well PP–III–003; Vargas–Cuervo, 2004). In this core, the San Andrés Formation reaches 113 m in thickness, although seismic information suggests that this carbonate unit is ca. 250 m thick. According to Bürgl (1959), the San Andrés Formation corresponds to lagoon and reefal deposits characterized by mudstones, wackestones, and packstones. Red algae and mollusks constitute the main allochems (Bürgl, 1959; Hubach, 1956). The San Andrés Formation has been correlated to the Providencia Formation (Providencia Island), the Martinez Reef Formation from the Nicaragua Rise, and the White Limestone from Jamaica (Geister, 1992).

3.4. Pleistocene and Recent Carbonates

3.4.1. La Popa Formation

According to Barrera (2001), the first reference of the name La Popa is found as La Popa Group in Anderson (1926 in Barrera, 2001), but the origin of this name as La Popa Formation was first used in a description by Bürgl (1957 in Barrera, 2001) of the strata constituting La Popa Hill in Cartagena. La Popa Formation emerges on a series of less abrupt and elongated hills between Cartagena and Barranquilla. The lithology is composed of solid clays that gradually pass upwards to reefal limestones. The age of this unit has been very controversial. However, Barrera (2001) postulates, based on the stratigraphic position and the microfauna recently collected by Servicio Geológico Colombiano, a Pleistocene age for this unit.

La Popa Formation was recently studied in one slim–hole stratigraphic well (Z well) along the Luruaco Anticlinorium of the SJDB (Figure 6b; Reyes et al., 2009). In this well, La Popa Formation consists of a basal siliciclastic unit and an upper carbonate unit (ca. 25 m thick). Carbonates from La Popa Formation consist of interbedded aggradational packages of framestones, grainstones, packstones, wackestones, and mudstones (Figure 16a). The framestones usually consist of different associations of massive corals in life position. The grainstones usually display fragments of massive corals as well as fragments of brachiopods, bivalves, gastropods, and green algae. Fragments of corals, gastropods, and echinoderms constitute the main allochemical components of the wackestones (Figure 16b–d). The interbedded siltstones are fossiliferous (fragments of bivalves, gastropods, green algae) and display parallel planar laminations, as well as moderate bioturbation.

Carbonates from La Popa Formation display $^{87}Sr/^{86}Sr$ values of 0.709097 and 0.709122 (Figure 7). These values suggest a Pleistocene depositional age for La Popa Formation. These ages partially overlap the ages proposed by Barrera (2001).

3.4.2. San Luis Formation

The Pleistocene San Luis Formation crops out in the San Andres Island, Colombia, along the Los Cayos Basin of the Lower Nicaragua Rise (Figure 6a). It was first described by Hubach (1956) and later on defined by Geister (1973, 1975). According to Geister (1973), the San Luis Formation is 15 m thick and mainly consists of biogenic packstones and grainstones. Corals constitute the main allochems of the San Luis Formation limestones. The Pleistocene depositional age of the San Luis Formation was obtained by Geister (1973), who used radiocarbon dating of carbonate remains.

3.5. Modern Marine Carbonate Areas of Colombia

Modern Colombian marine carbonate areas occur along the Colombian Caribbean continental shelf and as part of oceanic (Caribbean and Pacific) coral reef areas (Figure 17). These marine carbonate areas include several types of coral reef ecosystems and their interactions with other strategic ecosystems such as sea grass meadows and mangroves (Díaz et al., 2000, 2003), because all of them contain several coral species and other calcifying organisms. These areas cover approximately 2860 km^2. Most of these areas (76.5%) correspond to the San Andrés and Providencia Archipelago, where isolated carbonate platforms occur, characterized by the presence of fringing and barrier reefs, pinnacles, and atolls dominated by photozoans (corals) (Díaz et al., 2000; Instituto de Hidrología, Meteorología y Estudios Ambientales (IDEAM), 2017). Although the archipelago is located near the Central American continental shelf, it is affected by the Western Caribbean Current, the cyclonic Panamá–Colombia Gyre and its countercurrent, and the Magdalena River discharges (Criales et al., 2002), which prevent the Central American siliciclastic input from reaching the carbonate systems. The combination of these particular features allows the occurrence of euphotic and oligotrophic marine conditions,

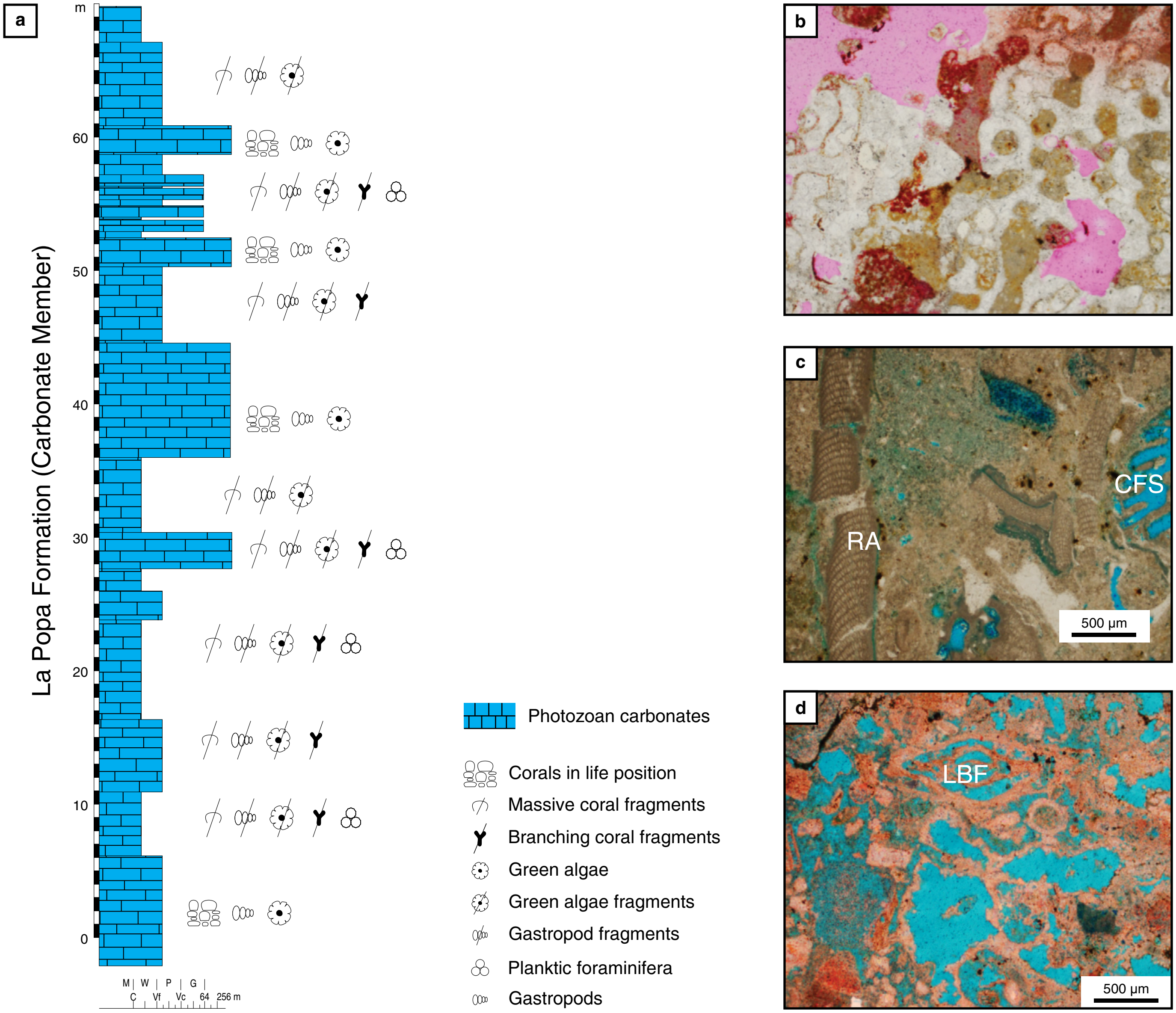

Figure 16. (a) Generalized lithostratigraphic column of La Popa Formation at well Y. **(b)** Photomicrography of a coral fragment from the upper part of La Popa Formation. **(c)** Photomicrography of wackestone from the lower part of La Popa Formation displaying red algal fragments (RA) and shadows of coral fragments (CFS). **(d)** Photomicrograph of limestone from the lower–most part of La Popa Formation displaying vuggy porosity and shadows of larger benthic foraminifera (LBF).

which in turn promote the preservation of a predominantly photozoan carbonate factory.

The second largest concentration of marine carbonate sedimentary areas occurs in the central sector of the Colombian Caribbean coast and its continental shelf (Figure 17). The San Bernardo and Rosario Archipelagos, the Tortuguilla and Fuerte Islands, and the Salmedina, Tortugas, and Bushnell lows, among others, are carbonate sedimentary successions that deposit on top of a series of topographic highs at the bottom of the continental shelf (Barrios, 2000; Díaz et al., 2000; Garzón–Ferreira et al., 2001). Modern carbonate sedimentary areas occur along portions of the coast with alternating coves or bays with rocky cliffs. This is the case for Urabá, near the border with Panamá, Santa Marta, and Parque Nacional Natural Tayrona. In these areas, algal rugs, coral reefs, beach rocks, meadows of seagrass, and sand plains occur. At the northern end of Colombia, on the shores of La Guajira Peninsula, similar areas also occur, which are mostly dominated by coral formations of limited extent (Díaz et al., 2000).

The Pacific continental and Oceanic marine areas display the least extensive carbonate sedimentation areas. While the continental areas are dominated by fringing and patchy coral reefs, those of the oceanic areas are dominated by fringing coral reefs and coralline biostromes. The development of coral reefs

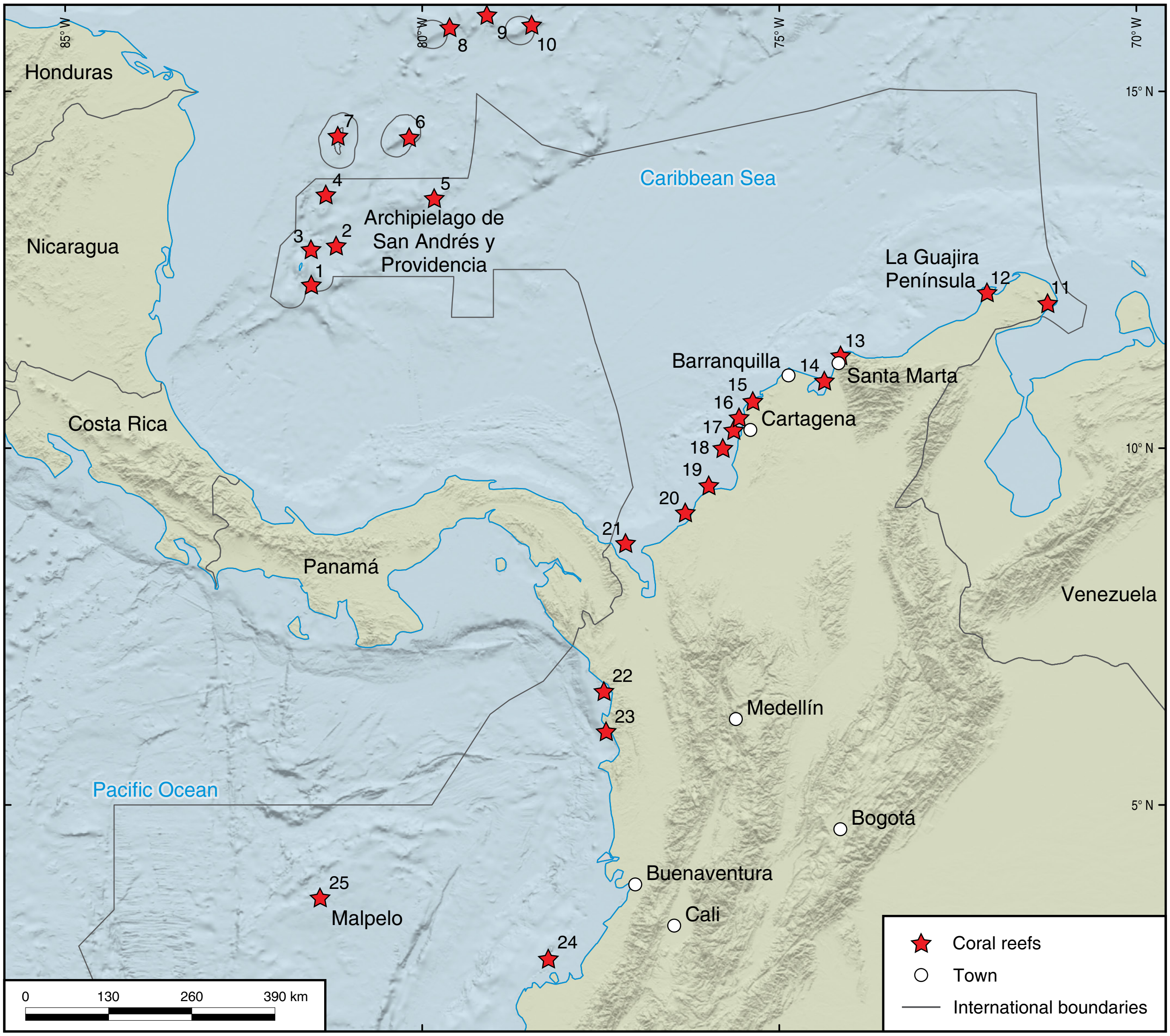

Figure 17. Locations of modern marine carbonate areas (coral reefs) in Colombia. Colombian coral reef areas: (1) Albuquerque Cay; (2) Courtown Cay; (3) San Andres Island; (4) Providence Island; (5) Roncador Bank; (6) Serrana Bank; (7) Quitasueño Bank; (8) Serrana Bank; (9) Alicia Bank; (10) Nuevo Cay; (11) Puerto López; (12) La Vela Bank; (13) Parque Nacional Natural Tayrona; (14) Banco de las Ánimas; (15) Santa Marta; (16) Salmedina Bank; (17) Rosario Island; (18) Tortuga Bank; (19) San Bernardo Island; (20) Tortuguilla Island; (21) Capurgana; (22) Cupica; (23) Utría; (24) Gorgona; (25) Malpelo. Modified from Barrios (2000) and Díaz et al. (2000).

in the Colombian Pacific follows the observed pattern for other tropical eastern Pacific coral reef formations (Barrios, 2007).

4. Evolution of the Carbonate Factories

Figure 18 presents a proposed model of the evolution of the Cenozoic carbonate factories from Colombia. The oldest Cenozoic shallow–water carbonate records correspond to the middle Eocene Arroyo de Piedra Formation (northern portion of the SJDB). It mainly consists of rhodolith packstones and rudstones. These carbonate facies display red algae and LBF as the main allochemical components (Salazar–Franco et al., 2016). The allochemical composition, together with the presence of claystone–siltstone intraclasts and interbedded calcareous mudstones and siltstones suggest that the Arroyo de Piedra Formation was deposited in three coeval environments: (1) Middle–proximal ramp rhodolith beds; (2) outer ramp/slope channels and lobes, mainly fed from the middle–ramp carbonate factory; and (3) outer ramp/slope open marine areas developed during a regional transgression (Figure

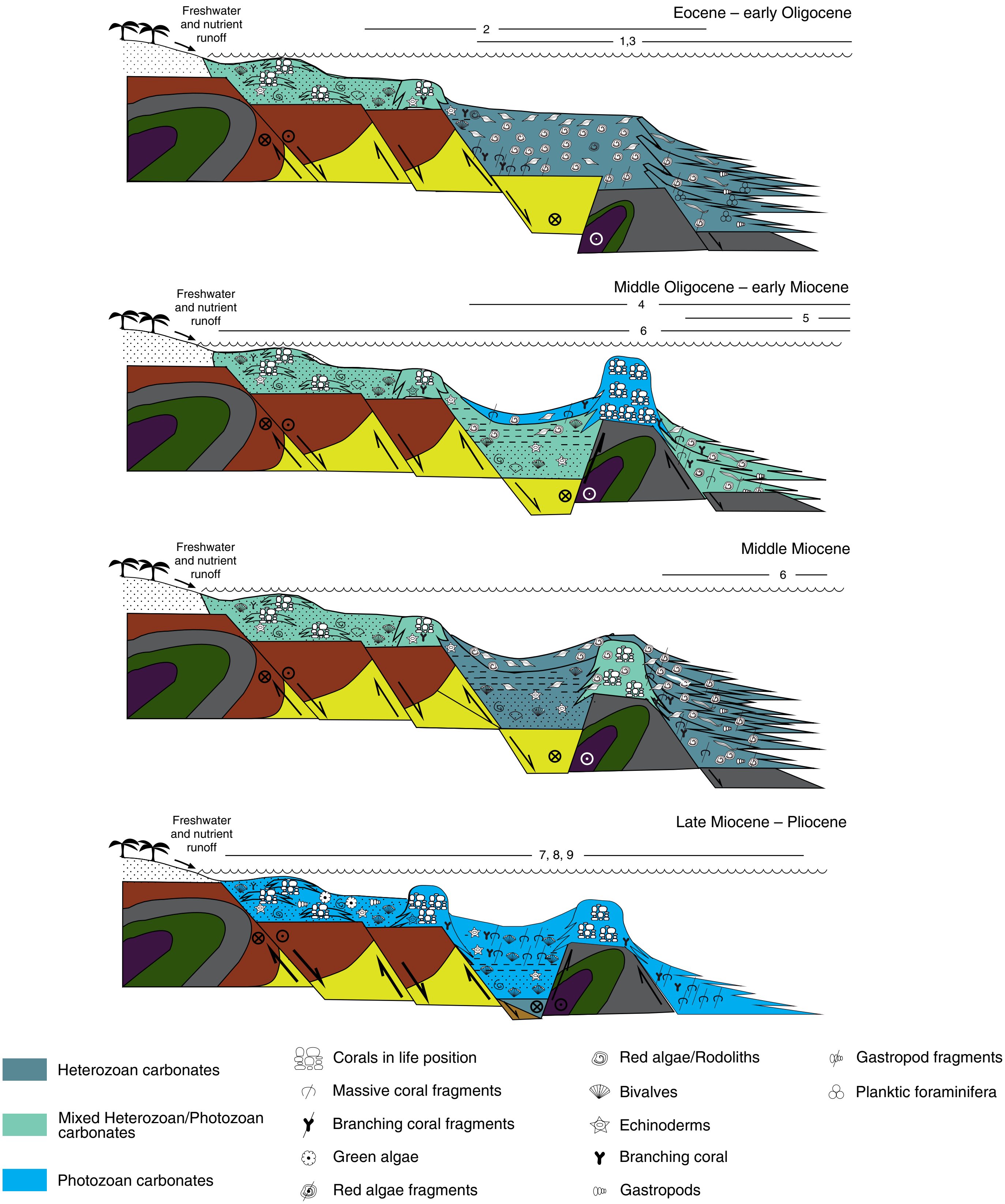

Figure 18. Schematic evolution of the Cenozoic shallow marine carbonate factories in Colombia. Numbers designate the range of variation in depositional style for each of the studied carbonate units. (1) Arroyo de Piedra Formation; (2) Toluviejo Formation; (3) Macarao Formation; (4) Cicuco Limestones; (5) Vijes Formation; (6) Siamana Formation; (7–9) San Andrés, San Luis, and La Popa Formations.

18). Transgressive–highstand systems are represented by the middle–proximal carbonate factory, while lowstand systems are characterized by the presence of reworked calcareous sedimentites. Transgressive events are characterized by the presence of open–sea facies (Figure 8; Salazar–Franco et al., 2016). The heterozoan biotic associations that characterize the carbonate factory of the Arroyo de Piedra Formation suggest a deposition under nutrient–rich (mesotrophic) oligophotic–to–mesophotic marine conditions.

Heterozoan biotic associations are also recorded in the central part of the SJDB, at the base of the Toluviejo Formation in the P8 well (Bermúdez et al., 2009). There, the carbonates of the Toluviejo Formation consist of wackestones and packstones, rich in red algal rhodoliths, which represents an initial carbonate deposition, which occurred during a period of relative sea level rise (Figure 10). A second transgressive cycle begins with the deposition of LBF grainstones and packstones, rich in red algal rhodoliths and LBF, as well as boundstones, rich in sponges and coral fragments, and it is also observed in the Porvenir Hill (Figure 10b; Ortiz et al., 1998). Such a biotic composition significantly differs from that observed in the Arroyo de Piedra Formation, where calcareous red algae are the dominant components. The significant abundance of LBF followed by red algae and the subordinate presence of coral fragments suggest the coexistence of both photozoan and heterozoan carbonates. The biotic association indicates clear, warm, oligotrophic waters, with a very low contribution of siliciclastic material (Tucker & Wright, 1990). These sedimentologic features of the Toluviejo carbonate factory, together with the presence of carbonate rich siltstones and claystones, suggest deposition along a shallow restricted platform, on which lagoon, patch reef, and tidal bar depositional environments coexisted (Figure 18; Ortiz et al., 1998).

The transgressive deepening tendency of the calcareous system in the Toluviejo Formation is followed by a regressive shallowing cycle, characterized by the presence of wackstones displaying a heterozoan biotic association that normally develops under nutrient–rich (mesotrophic), oligophotic–to–mesophotic marine conditions (oncoids, mollusks, and echinoderms; Figure 10). The switch in the biotic community might be the effect of the shallowing cycle, which includes the progressive inclusion of detrital material, increased nutrient availability, and increased turbidity of the water. The presence of river systems adding sediment to the continental shelf is supported by the lateral occurrence of calcareous mudstones from the Chengue Formation, which have been interpreted as deposition along a deep inner mixed siliciclastic–carbonate shelf (Bermúdez et al., 2009; Guzmán, 2007).

During the late Eocene, the heterozoan biotic associations constituted the dominant carbonate factory along the Alta Guajira Basin (Macarao Formation). The presence of coralline algae and LBF (mainly *Nummulites* and lepidocyclinids) suggests deposition under oligophotic–to–mesophotic and nutrient–rich (mesotrophic) marine conditions. The aggradational stacking pattern of the studied carbonates together with the presence of thick aggradational massive quartz sandstones suggests that the carbonate successions of the Macarao Formation were also deposited as rhodalgal biostromes along a mixed siliciclastic–carbonate shelf (Figure 18; Tucker & Wright, 1990).

The middle Oligocene to lower Miocene carbonates from the Cicuco Limestones (Ciénaga de Oro Formation) at the Lower Magdalena Valley exhibit a facies association typical of rimmed carbonate shelves (Figures 11, 18). The presence of red alga–rich packstones and grainstones with low terrigenous content is interpreted as isolated carbonate banks (patch–reefs of coralline algae) deposited on top of basement heights. The presence of red algal bioclastic grainstones, wackestones, and packstones, rich in siliciclastic debris suggests a deposition along a back–reef sandy belt of coralline algae (Ortiz & Niño, 1999). This proposal is supported by the occurrence of mixed heterozoan–photozoan biotic associations consisting of crustose coralline algae (*Melobesieae*), LBF (Camerinidae, Orbitoididae), sponges (Calcispongea), corals, and mollusks (Pelecypoda). The predominance of heterozoan biotic associations over photozoan biotic associations suggests that the deposition of carbonates occurred under mesotrophic marine conditions. The basal coarsening upward carbonates (Figure 11), deposited at the base of these paleo–highs, evidence a transgressive system that gradually evolves towards a highstand, which occurs when the rate of sea level rise decreases, allowing the establishment of reef facies and shelf edge deposits that prograde seaward. Finally, the siliciclastic contributions observed at the top of the limestones suggest a lowstand event that, in some, cases led to the burial of the carbonates and in others to subaerial exposure.

To the southwest, in the eastern flank of the Western Cordillera, and during the Oligocene, the carbonate factory of the Vijes Formation consists of heterozoan biotic associations. The presence of LBF, bivalves, echinoderms, gastropods, bryozoans, calcareous red algae, and oncolites suggests a deposition under dimmed (oligophotic/aphotic) and highly mesotrophic marine conditions. The fining–upward staking patterns of the studied carbonates along with the presence of interbedded massive sandstones suggest a deposition along rimmed carbonate banks developed along the shelves of the Western Cordillera of the Colombia volcano–sedimentary basement (Figure 18).

The lowermost part of the Siamana Formation, deposited during the late Oligocene, displays facies associations typical of mixed siliciclastic/carbonate shelves. The mixed heterozoan–photozoan carbonate factory consists of bivalves, gastropods, echinoderms, corals, and LBF. The mixed carbonate factory occurs as isolated carbonate banks (i.e., patchy coral reefs) deposited on top of basement heights, which laterally change towards siliciclastic fan deltas (Figure 18). The decrease in siliciclastic material with section height along with the decrease in the occurrence of heterozoan biotic associations marks a shift in depositional style from a mixed siliciclastic–carbonate shelf into a predominant carbonate shelf, in which unrimmed carbonate banks are detached from the siliciclastic continental shelf (Figure 18). The middle part of the Siamana Formation, deposited during the early Miocene, mostly displays tabular aggradational packages of floatstones, rudstones, framestones, packstones, and grainstones. The dominance of coral fragments, benthic foraminifera, and red algae, along with the decrease in siliciclastic material, also suggest deposition along a detached/unrimmed carbonate bank dominated by coral reefs (Figure 18). The absence of siliciclastic material and predominance of massive corals in the hundreds–of–meters–wide framestones, floatstones, and rudstones, suggest that the predominant photozoan carbonate factory developed under oligotrophic/euphotic marine conditions. The predominance of photozoan biotic associations over heterozoans biotic associations suggest that the deposition of carbonates from the middle part of the Siamana Formation occurred under low mesotrophic marine conditions.

The upper part of the Siamana Formation (early – middle Miocene) exhibits two main intervals of highly diverse coral–dominated tabular and aggradational framestones, rudstones, and floatstones. These characteristics suggest important changes in the carbonate factory from mixed photozoan–heterozoan–dominated to mostly photozoan–dominated biotic assemblages (Figure 18). The presence of diverse coral reefs in the kilometer–wide framestone/rudstone/floatstone intervals suggests that deposition along fringing reef systems in isolated rimmed carbonate platforms developed along the continental shelf. The development of these coral reefs was favored by the absence of sediment supply from the continental shelf and occurrence of oligotrophic and euphotic marine conditions. The uppermost part of the Siamana Formation displays a series of tabular thick–bedded packstones and grainstones, as well as biostromes, which consist of red algae, rhodoliths, and benthic and planktic foraminifera. The change in the carbonate factory from a photozoan–dominated to a heterozoan–dominated biotic association suggests an important change in the environmental conditions from oligotrophic to mesotrophic conditions. This change was likely associated with an increase in the siliciclastic sediment supply to the continental shelf along the Cocinetas Sub–basin.

The Pleistocene carbonates of La Popa Formation display sedimentary facies that have been interpreted as fringing reefs (Reyes et al., 2009). The mixed carbonate factory is composed of photozoan and heterozoan biotic associations. These biotic associations, along with the presence of aggradational packages of framestones, grainstones, packstones, and wackestones interbedded with calcareous mudstones, suggest deposition along carbonate banks attached to the continental shelf (Figure 18). The presence of corals, brachiopods, bivalves, gastropods, and green algae suggest a wide range of photic conditions (from euphotic to aphotic), as well as deposition under oligotrophic and low mesotrophic marine conditions. Modern coral reefs in the area grow on carbonates from La Popa Formation (Díaz et al., 2000), and the variety of associated flora and fauna resemble the conditions of the ancient coral reef formations.

5. Processes Controlling Temporal Changes in the Colombian Eocene – Miocene Shallow Marine Carbonate Factories

The evolution of several Cenozoic sedimentary basins in northern South America has been influenced by the interaction of different tectonic blocks (i.e., the Central and South American Blocks and the Caribbean and Nazca Plates) (Cediel et al., 2003). An important tectonic event that influenced the evolution of the Cenozoic sedimentary basins in northern South America is the middle Eocene initial interaction between Central America and South America (Farris et al., 2011; Montes et al., 2012). This event, which caused the opening of several middle Eocene marginal basins, was followed by the onset of low–angle flat subduction of the Caribbean Plate under the South American Plate during the late Eocene – Oligocene interval (Mora et al., 2017). This tectonic reorganization resulted in fore–arc extension and enhanced subsidence, and siliciclastic sedimentation along several of the middle Eocene incipient marginal basins in northern South America. In the San Jacinto and Alta Guajira Basins, these conditions favored the coeval occurrence of late Eocene coarse–grained clastic and shallow marine carbonate sedimentation (Mora et al., 2017). The increase in sediment and nutrient supply from the emerged orogens into these basins, amplified by the Eocene hothouse conditions (Zachos et al., 2001, 2008), could be a mechanism to explain the predominance of heterozoan biotic associations over photozoan biotic associations as the main carbonate factory along the studied Colombian Cenozoic basins (i.e., Arroyo de Piedra Formation of the San Jacinto Basin and Macarao Formation of the Alta Guajira Basin; Figure 19). An alternative mechanism triggering the predominance of middle – late Eocene heterozoan carbonate factories could be the occurrence of local coastal upwelling currents, which cause local drops in sea surface temperatures while increasing the delivery of high nutrient loads to shallow waters (Figure 19). The occurrence of upwelling currents would have been enhanced by the early closure of the Panamá Isthmus, which also invigorated the west boundary current along the Caribbean (Schmidt, 2007).

During the middle Oligocene – early Miocene interval, several intramountain sedimentary basins experienced increased subsidence in the northern Andes (Montes et al., 2015; Mora et al., 2010; Silva–Tamayo et al., 2008). These basins acted as main catchment of sediments derived from the Eocene–uplifted

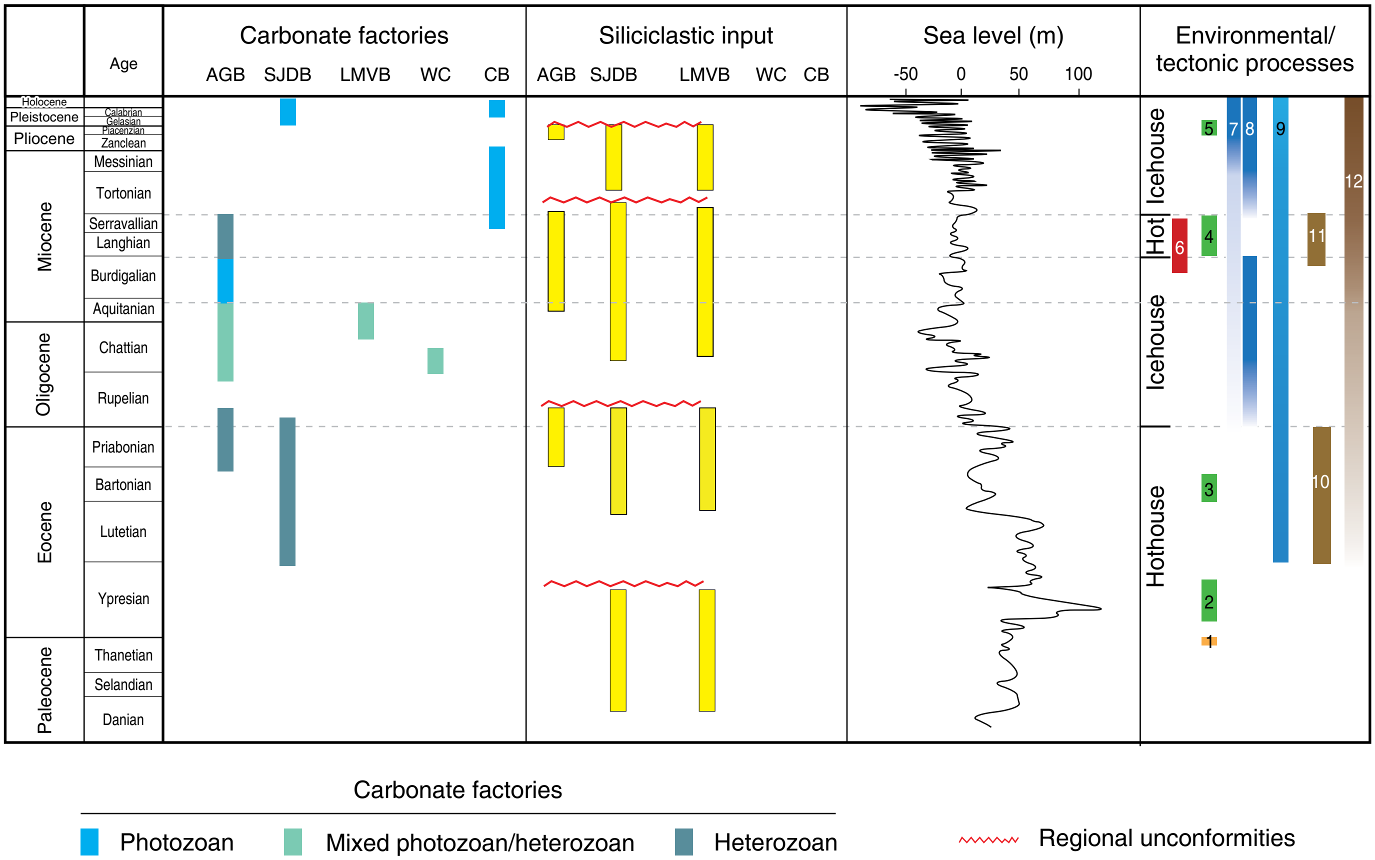

Figure 19. Evolution of the Cenozoic carbonate factories along the: (AGB) Alta Guajira Basin; (SJDB) San Jacinto deformed belt of the San Jacinto Basin; (LMVB) Lower Magdalena Valley Basin; (WC) Western Cordillera of Colombia; (CB) Los Cayos Basin. The occurrence of siliciclastic input into the different basins is subsequently constrained (Bermúdez et al., 2009; Dueñas et al., 2000; Moreno et al., 2015; Reyes–Harker et al., 2000; Silva–Tamayo et al., 2017; Vargas–Cuervo, 2004). Cenozoic sea level curve after Miller et al. (2005) and Zachos et al. (2001, 2008). The major Cenozoic environmental processes are as follows: (1) Paleocene – Eocene Thermal Maximum; (2) middle Eocene Climate Optimum; (3) late Eocene Climate Optimum; (4) middle Miocene Climate Optimum; (5) late Pliocene Climate Optimum; (6) Monterrey event; (7) Northern Hemisphere glacier formation; (8) Southern Hemisphere glacier formation; (9) strength of the west boundary current. The major tectonic events along northern South America are as follows: (10) Initial interaction between Central and South America; (11) final docking of Central America to South America; (12) Andean orogeny.

orogens (Montes et al., 2015; Mora et al., 2010), resulting in a decrease in the sediment supply to the continental shelves and, thus, in either a lack of deposition or reduced siliciclastic sedimentation in the marginal basins (Figure 19). The decreased sediment supply to the continental shelves, along with the decrease in global temperatures and sea level (Miller et al., 2005; Zachos et al., 2001, 2008), explains the occurrence of mixed photozoan–heterozoan biotic associations in the Alta Guajira (Siamana Formation), Lower Magdalena Valley (Ciénaga de Oro Formation), and Western Cordillera of Colombia (Vijes Formation) (Figure 19). These environmental conditions would have continued during the early Miocene, accounting for the development of highly diverse coral reefs in the Alta Guajira Basin and in general along the Circum–Caribbean (Budd, 2000).

Montes et al. (2015) proposed that final exhumation of the Panamá Isthmus occurred by the middle Miocene (Figure 18). The Langhian–Serravallian tectonic interaction between Panamá and northern South America would have, conversely, enhanced the uplift of the Northern Andes (Mora et al., 2010; Restrepo–Moreno et al., 2009; Villagómez et al., 2011), resulting in a high sediment supply to both the Caribbean and the Pacific. The enhanced sediment supply to the Caribbean would have increased ocean water turbidity. The increase in nutrient availability along the Caribbean together with the combined action of the increased sediment supply from the emerged Andes and Panamá Isthmus would have further favored the proliferation of calcareous alga–rich carbonates during this time and the decrease in coral diversity (Figure 19), as calcareous algae are more resistant to turbidity and high influxes of nutrients than corals (Halfar & Mutti, 2005). The occurrence of widespread middle Miocene calcareous alga successions along the Caribbean and the concomitant disappearance of coral reef successions ultimately suggest that enhanced sediment influxes during the middle Miocene (Budd, 2000) would have been another causal effect of the changes in the carbonate factories, due to deteriorating ocean water conditions.

The late Miocene – early Pliocene interval witnessed a decrease in the occurrence of marine carbonates along with an increase in coral biodiversity in the Circum–Caribbean (Johnson et al., 2008). The San Andrés Formation in Los Cayos Basin, however, displays high coral diversity. This could have been associated with the onset of free–living solitary and flabelo–meandroid corals (Klaus et al., 2011), and the appearance of *Acropora*–dominated coral reefs during the Miocene – Pliocene transition (McNeill et al., 1997), which marks an important change in coral adaptation to the adverse oceanographic conditions along the Circum–Caribbean modulated by rapid fluctuations in sea level (Renema et al., 2016). The onset of *Acropora*–dominated coral reefs during the early Pliocene would explain the successful occurrence of highly diverse coral reefs in La Popa and San Luis Formations during a period of deteriorated regional environmental conditions, i.e., enhanced sediment supply (Figure 19).

The prolonged period of reef coral species origination that took place between the late Miocene and early Pliocene (Budd & Johnson, 1999) was followed by sequential extinctions of shallow–water species throughout the Pliocene and deeper water corals in the middle Pleistocene (Getty et al., 2001; Maier et al., 2007). Currently, algae are the most abundant biotic component in nearly all coral reefs of Colombia, ranging from 30% in Rosario Islands to 53% in the San Andrés Archipelago (Rodríguez–Ramírez et al., 2010). Temporal analyses suggest a loss of coral covering *Acropora palmata*, as well as an increased algal cover, particularly in Rosario Islands (Rodríguez–Ramírez et al., 2010). In addition to modern natural disturbances, such as hurricanes, bleaching events, and epidemic diseases, which can also be the indirect result of human activities, factors directly linked to anthropogenic disturbances (high sea surface temperatures, sedimentation, and turbidity) have been defined as the main causes of this environmental change (Restrepo & Alvarado, 2001). Similar to other Caribbean localities, it is highly likely that most near–shore coral reef environments are doomed to further decline under the increasing human population and predicted future climate change scenarios, which may result in prolonged sea surface warming, massive coral bleaching, and extreme weather events accompanied by increased runoff impacts to the coastal areas (Restrepo et al., 2016).

6. Conclusions

Detailed stratigraphy and Sr–isotope dating of several shallow marine carbonate successions from different Colombian basins allowed the linking of major variation in the SE Circum–Caribbean Cenozoic carbonate factories to major regional environmental changes. Predominantly heterozoan biotic associations constituted the main carbonate factory along the San Jacinto and Alta Guajira Basins during the middle – late Eocene and middle Miocene intervals. The occurrence of calcareous alga–dominated factories resulted from increased marine upwelling and enhanced sediment delivery to the SE Circum–Caribbean as the Panamá Isthmus emerged above sea level and the Northern Andes experienced enhanced uplift. Photozoan biotic associations, dominated by corals, constituted the main shallow carbonate factory during the middle Oligocene – early Miocene interval. The occurrence of these carbonate factories was restricted to the Alta Guajira Basin, Lower Magdalena Valley Basin, and Western Cordillera of Colombia. The occurrence of coral reef–dominated factories during the middle Oligocene – early Miocene interval paralleled the onset of the Antarctic glaciations and a decrease in sediment supply to the Caribbean Basin. The continental margin of northern South America registered a lack of marine carbonate deposition during the late Miocene – late Pliocene interval, which was related to the increase in siliciclastic sedimentation into the SE Circum–Caribbean. This decrease in occurrence of carbonate successions was interrupted by a single episode of carbonate sedimentation (La Popa Formation) along the San Jacinto Basin during the Pleistocene. This episode of carbonate deposition was related to the onset of Acropora–dominated coral reefs along the Caribbean, which successfully flourished during a period of rapid fluctuations in sea level. The adverse local environmental conditions that affected the late Miocene – Pleistocene carbonate sedimentation along the continental margin did not affect Los Cayos Basin, where highly diverse coral–dominated carbonate successions occur.

Acknowledgments

This work was supported by the financial aid of the Empresa Colombiana de Petróleo and the research office from the Universidad de Caldas, Manizales, Colombia (Grants VIP 0025311 and VIP 0027411 to Juan Carlos SILVA–TAMAYO and Andrés PARDO–TRUJILLO). The work favored access to slims–hole cores from the Agencia Nacional de Hidrocarburos. Juan Carlos SILVA–TAMAYO is thankful to the Smithsonian Tropical Research Institute for providing financial support through a postdoctoral scholarship sponsored by the Empresa Colombiana de Petróleo. Juan Carlos SILVA–TAMAYO is also thankful with Testlab Laboratorio Analisis Alimentos y Aguas S.A.S. for providing additional funding. The authors are thankful to James S. KLAUS and an anonymous reviewer for their comments, which greatly improved the quality of the manuscript.

References

Alfonso, M., Herrera, J.M., Navarrete, R.E., Bermúdez, H.D., Calderón, J.E., Parra, F.E., Sarmiento, G., Vega, F. & Perrilliat, M. 2009. Cartografía geológica, levantamiento de columnas estratigráficas, toma de muestras y análisis bioestratigráficos.

Sector de Chalán, Cuenca Sinú–San Jacinto. ANH–ATG, unpublished report, 120 p. Bogotá.

Barrera, R. 2001. Memoria explicativa: Geología de las planchas 16 Galerazamba y 17 Barranquilla. Scale 1:100 000. Ingeominas, 54 p. Bogotá.

Barrios, L.M. 2000. Evaluación de las principales condiciones de deterioro de los corales pétreos en el Caribe colombiano. Master thesis, Universidad Nacional de Colombia. 144 p. Santa Marta, Colombia.

Barrios, L.M. 2007. Taxonomy and general ecology of marine invertebrates from Las Perlas Archipelago, Panamanian tropical eastern Pacific. Doctoral thesis, Heriot–Watt University, 218 p. Edinburgh, UK.

Bermúdez, H.D., Grajales, J.A., Restrepo, L.C. & Rosero, J.S. 2009. Estudio Integrado de los núcleos y registros obtenidos de los pozos someros tipo "slim holes" en la Cuenca Sinú. Informe final, Tomo 1. ANH–Universidad de Caldas, 73 p. Bogotá.

Budd, A.F. 2000. Diversity and extinction in the Cenozoic history of Caribbean reefs. Coral Reefs, 19(1): 25–35. https://doi.org/10.1007/s003380050222

Budd, A.F. & Johnson, K.G. 1999. Origination preceding extinction during late Cenozoic turnover of Caribbean reefs. Paleobiology 25, 188–200. https://doi.org/10.1017/S009483730002649X

Bueno, R. 1970. Eleventh Field Conference: The geology of the Tubará region, Lower Magdalena Basin. In: Colombian Society of Petroleum Geologists and Geophysicists, Geological Field Trips Colombia 1959–1978. Ediciones Geotec Ltda, p. 299–324. Bogotá.

Bürgl, H. 1959. Resumen de la estratigrafía de Colombia. Servicio Geológico Nacional, Internal report 1248, 18 p. Bogotá.

Cediel, F., Shaw, R.P. & Cáceres, C. 2003. Tectonic assembly of the northern Andean Block. In: Bartolini, C., Buffler, R.T. & Blickwede, J. (editors), The circum–Gulf of Mexico and the Caribbean: Hydrocarbon habitats, basin formation, and plate tectonics. American Association of Petroleum Geologists, Memoir 79, p. 815–848. Tulsa, USA.

Criales, M.M., Yeung, C, Amaya, F. López, A., Jones, D.L. & Richards, W.J. 2002. Larval supply of fishes, shrimps, and crabs into the nursery ground of the Ciénaga Grande de Santa Marta, Colombian Caribbean. Caribbean Journal of Science, 38(1–2): 52–65.

Díaz, J.M., Barrios, L.M., Cendales, M.H., Garzón–Ferreira, J., Geister, J., López–Victoria, M., Ospina, G.H., Parra–Velandia, F., Pinzón, J., Vargas–Ángel, B., Zapata, F.A. & Zea, S. 2000. Áreas coralinas de Colombia. Invemar, Publicaciones Especiales (5), 176 p. Santa Marta, Colombia.

Díaz, J.M., Barrios, L.M. & Gomez, D.I., editors. 2003. Las praderas de pastos marinos en Colombia: Estructura y distribución de un ecosistema estratégico. Invemar, Publicaciones Especiales (10), 163 p. Santa Marta, Colombia.

Ducea, M. & Saleeby, J. 1998. A case for delamination of the deep batholithic crust beneath the Sierra Nevada, California. International Geology Review, 40(1): 78–93. https://doi.org/10.1080/00206819809465199

Dueñas, H. 1977. Estudio palinológico del pozo Q–E–22 Oligoceno Superior a Mioceno Inferior, Planeta Rica, Norte de Colombia. Boletín Geológico, 22(3): 96–115.

Dueñas, H. 1986. Geología y palinología de la Formación Ciénaga de Oro, región Caribe colombiana. Publicaciones Geológicas Especiales del Ingeominas (18): p. 1–64. Bogotá.

Dueñas, H., Navarrete, R.E., Mojica, J., Pardo, M. & Camargo, R. 2000. Edad de la Formación Vijes en el pozo V3A, Oligoceno del piedemonte oriental de la cordillera Occidental, departamento del Valle del Cauca, Colombia. Geología Colombiana, (25): 25–43.

Dunham, R.J. 1962. Classification of carbonate rocks according to depositional texture. In: Ham, W.E. (editor), Classification of carbonate rocks, American Association of Petroleum Geologists, Memoir 1, p. 108–121. Tulsa, USA.

Duque–Caro, H. 1968. Observaciones generales a la bioestratigrafía y geología regional en los departamentos de Bolívar y Córdoba. Boletín de Geología (24): 71–87.

Duque–Caro, H. 1975. Los foraminíferos planctónicos y el terciario de Colombia. Revista Española de Micropaleontología, 7(3): 403– 427

Embry, A.F. & Klovan, E.J. 1971. A late Devonian reef tract of northeastern Banks Island, N.W.T. Bulletin of the Canadian Petroleum Geology, 19(4): 730–781.

Farris, D.W., Jaramillo, C., Bayona, G., Restrepo–Moreno, S.A., Montes, C., Cardona, A. & Mora, A., Speakman, R.J., Glascock, M.D. & Valencia, V. 2011. Fracturing of the Panamanian Isthmus during initial collision with South America. Geology, 39(11): 1007–1010. https://doi.org/10.1130/G32237.1

Frost, S.H. 1977. Cenozoic reef systems of the Caribbean: Prospects for paleoecologic synthesis. In: Frost, S.H., Weiss, M.P. & Saunders, J.B. (editors), Reefs and related carbonates: Ecology and sedimentology. American Association of Petroleum Geologists, 4: p. 93–110. Tulsa, USA. https://doi.org/10.1306/St4393C8

Garzón–Ferreira, J., Gil–Agudelo, D.L., Barrios, L.M. & Zea, S. 2001. Stony coral diseases observed in southwestern Caribbean reefs. Hydrobiologia, 460(1–3): 65–69.

Geister, J. 1973. Los arrecifes de la isla de San Andrés. Mitteilungen aus dem Instituto Colombo–Alemán de Investigaciones Científicas, 7: p. 211–228. Santa Marta, Colombia.

Geister, J. 1975. Riffbau und geologische entwicklungsgeschichte der insel San Andrés, westliches Karibisches Meer, Kolumbien. Stuttgarter Beiträge zur Naturkunde, Geologie und Paläontologie, (15): p. 1–203. Stuttgart, Germany.

Geister, J. 1992. Modern reef development and Cenozoic evolution of an oceanic island/reef complex: Isla de Providencia, western Caribbean Sea, Colombia. Facies, 27(1): 1–70.

Getty, S.R., Asmerom, Y., Quinn, T.M. & Budd, A.F. 2001. Accelerated Pleistocene coral extinctions in the Caribbean Basin shown by uranium–lead (U–Pb) dating. Geology, 29(7):

639–642. https://doi.org/10.1130/0091-7613(2001)029<0639:APCEIT>2.0.CO;2

Guzmán, G. 2007. Stratigraphy and sedimentary environment and implications in the Plato Basin and the San Jacinto belt northwestern Colombia. Doctoral thesis, Université de Liège, 275 p. Liège, Belgium.

Guzmán, G., Gómez, E. & Serrano, B.E. 2004. Geología de los cinturones del Sinú, San Jacinto y borde Occidental del Valle Inferior del Magdalena, Caribe Colombiano. Scale 1:300 000. Ingeominas, internal report, 134 p. Bogotá.

Halfar, J. & Mutti, M. 2005. Global dominance of coralline red–algal facies: A response to Miocene oceanographic events. Geology 33(6): 481–484. https://doi.org/10.1130/G21462.1

Hubach, E. 1956. Aspectos geográficos y geológicos y recursos de las islas de San Andrés y Providencia. Cuadernos de Geografía de Colombia, (12): p. 1–37.

Instituto de Hidrología, Meteorología y Estudios Ambientales (IDEAM). 2017. Mapa de ecosistemas continentales, costeros y marinos de Colombia, versión 2.1. Scale 1:1 200 000. Bogotá. http://www.ideam.gov.co/documents/11769/222663/E_EC-CMC_Ver21_100K.pdf/addc175f-3ac6-415b-9b9e-a1c4368b-5b3e (consulted in December 2017).

Jacobsen, S.B. & Kaufman, A.J. 1999. The Sr, C and O isotopic evolution of Neoproterozoic seawater. Chemical Geology, 161(1–3): 37–57. https://doi.org/10.1016/S0009-2541(99)00080-7

James, N.P. & Jones, B. 2016. Origin of carbonate sedimentary rocks. John Wiley & Sons, 464 p. Chichester, UK.

Johnson, K.G., Jackson, J.B. & Budd, A.F. 2008. Caribbean reef development was independent of coral diversity over 28 million years. Science, 319(5869): 1521–1523. https://doi.org/10.1126/science.1152197

Johnson, K.G., Sánchez–Villagra, M.R. & Aguilera, O.A. 2009. The Oligocene – Miocene transition on coral reefs in the Falcón Basin, NW Venezuela. Palaios, 24(1–2): 59–69.

Kassem, T., Cáceres, C. & Cucalón, I. 1967. Memoria explicativa: Geología del Cuadrángulo E–8 Sincelejo. Servicio Geológico Nacional, unpublished report, 150 p. Bogotá.

Klaus, J.S., Lutz, B.P., McNeill, D.F., Budd, A.F., Johnson, K.G. & Ishman, S.E. 2011. Rise and fall of Pliocene free–living corals in the Caribbean. Geology, 39(4): 375–378. https://doi.org/10.1130/G31704.1

Lockwood, J.G. 1974. World climatology: An environmental approach. St. Marti's Press, 330 p. London, UK.

Maier, K.L., Klaus, J.S., McNeill, D.F. & Budd, A.F. 2007. A late Miocene low–nutrient window for Caribbean reef formation? Coral reefs, 26(3): 635–639. https://doi.org/10.1007/s00338-007-0254-6

McArthur, J.M. & Howarth, R.J. 2004. Sr–isotope stratigraphy: The Phanerozoic $^{87}Sr/^{86}Sr$–curve and explanatory notes. In: Gradstein, F., Ogg, J. & Smith, A.G. (editors), A Geological Time Scale 2004. Cambridge University Press, p. 96–105. Cambridge, UK. https://doi.org/10.1017/CBO9780511536045.008

McArthur, J.M., Howarth, R.J. & Shields–Zhou, G.A. 2012. Strontium isotope stratigraphy. In: Gradstein, F., Ogg, J., Schmitz, M. & Ogg, G. (editors), The Geologic Time Scale 2012. Elsevier, p. 127–144. Oxford, UK. https://doi.org/10.1016/B978-0-444-59425-9.00007-X

McNeill, D.F., Budd, A.F. & Borne, P.F. 1997. Earlier (late Pliocene) first appearance of the Caribbean reef–building coral *Acropora palmata*: Stratigraphic and evolutionary implications. Geology, 25(10): 891–894. https://doi.org/10.1130/0091-7613(1997)025<0891:ELPFAO>2.3.CO;2

Miller, K.G., Kominz, M.A., Browning, J.V., Wright, J.D., Mountain, G.S., Katz, M.E., Sugarman, P.J., Cramer, B.S., Christie–Blick, N. & Pekar, S.F. 2005. The Phanerozoic record of global sea–level change. Science, 310(5752): 1293–1298. https://doi.org/10.1126/science.1116412

Montes, C., Cardona, A., McFadden, R., Morón, S.E., Silva, C.A., Restrepo–Moreno, S., Ramírez, D.A., Hoyos, N., Wilson, J., Farris, D., Bayona, G.A., Jaramillo, C.A., Valencia, V., Bryan, J. & Flores, J.A. 2012. Evidence for middle Eocene and younger emergence in central Panamá: Implications for isthmus closure. Geological Society of America Bulletin, 124(5–6): 780–799. https://doi.org/10.1130/B30528.1

Montes, C., Cardona, A., Jaramillo, C., Pardo, A., Silva, J.C., Valencia, V., Ayala, C., Pérez–Ángel, L.C., Rodríguez–Parra, L.A., Ramírez, V. & Niño, H. 2015. Middle Miocene closure of the Central American Seaway. Science, 348(6231): 226–229. https://doi.org/10.1126/science.aaa2815

Mora, A., Horton, B.K., Mesa, A., Rubiano, J., Ketcham, R.A., Parra, M., Blanco, V., Garcia, D. & Stockli, D.F. 2010. Migration of Cenozoic deformation in the Eastern Cordillera of Colombia interpreted from fission track results and structural relationships: Implications for petroleum systems. American Association of Petroleum Geologists Bulletin, 94(10): 1543–1580. https://doi.org/10.1306/01051009111

Mora, J.A., Oncken, O., Le Breton, E., Ibañez–Mejía, M., Faccenna, C., Veloza, G., Vélez, V., de Freitas, M. & Mesa, A. 2017. Linking Late Cretaceous to Eocene tectonostratigraphy of the San Jacinto fold belt of NW Colombia with Caribbean Plateau collision and flat subduction. Tectonics 36(11): 2599–2629. https://doi.org/10.1002/2017TC004612

Moreno, J.F., Hendy, A.J.W., Quiroz, L., Hoyos, N., Jones, D.S., Zapata, V., Zapata, S., Ballen, G.A., Cadena, E., Cárdenas, A.L., Carrillo–Briceño, J.D., Carrillo, J.D., Delgado–Sierra, D., Escobar, J., Martínez, J.I., Martínez, C., Montes, C., Moreno, J., Pérez, N., Sánchez, R., Suárez, C., Vallejo–Pareja, M.C. & Jaramillo, C. 2015. Revised stratigraphy of Neogene strata in the Cocinetas Basin, La Guajira, Colombia. Swiss Journal of Palaeontology, 134(1): 5–43. https://doi.org/10.1007/s13358-015-0071-4

Mutti, M., Droxler, A.W. & Cunningham, A.D. 2005. Evolution of the northern Nicaragua Rise during the Oligocene – Miocene: Drowning by environmental factors. Sedimentary

Geology 175(1–4): 237–258. https://doi.org/10.1016/j.sedgeo.2004.12.028

Nivia, Á. 2001. Memoria explicativa: Mapa geológico departamento del Valle del Cauca. Scale 1:250 000. Ingeominas, 148 p. Bogotá.

Ortiz, A. & Niño, H. 1999. Estudio sedimentológico y estratigráfico de las calizas de Cicuco y Boquete en un sector de la isla de Mompós, Valle Inferior del Magdalena. Ecopetrol & Instituto Colombiano del Petróleo, unpublished report, 32 p. Bogotá.

Ortiz, A., Blanco, A. & Corredor, G. 1998. Calidad de reservorio de las calizas de las formaciones Toluviejo y Ciénaga de Oro, Subcuenca Sinú–San Jacinto, Cuenca Caribe Colombiana. Instituto Colombiano del Petróleo & Ecopetrol, unpublished report, 88 p. Bogotá.

Renema, W., Pandolfi, J.M., Kiessling, W., Bosellini, F.R., Klaus, J.S., Korpanty, C., Rosen, B.R., Santodomingo, N., Wallace, C.C., Webster, J.M. & Johnson, K.G. 2016. Are coral reefs victims of their own past success? Science Advances, 2(4), e1500850. https://doi.org/10.1126/sciadv.1500850

Renz, O. 1960. Geología de la parte sureste de la península de La Guajira (República de Colombia). III Congreso Geológico Venezolano. Memoirs, III, p. 317–346.

Restrepo, J.D. & Alvarado, E.M. 2011. Assessing major environmental issues in the Caribbean and Pacific coast of Colombia, South America: An overview of fluvial fluxes, coral reef degradation, and mangrove ecosystems impacted by river diversion. In: Wolanski, E., & McLusky, D.S. (editors), Treatise on estuarine and coastal Science. Academic Press, p. 289–314. Waltham, USA. https://doi.org/10.1016/B978-0-12-374711-2.01117-7

Restrepo, J.D., Park, E., Aquino, S. & Latrubesse, E.M. 2016. Coral reefs chronically exposed to river sediment plumes in the southwestern Caribbean: Rosario Islands, Colombia. Science of the Total Environment 553: 316–329. https://doi.org/10.1016/j.scitotenv.2016.02.140

Restrepo–Moreno, S.A., Foster, D.A., Stockli, D.F. & Parra–Sánchez, L.N. 2009. Long–term erosion and exhumation of the "Altiplano Antioqueño", northern Andes (Colombia) from apatite (U–Th)/He thermochronology. Earth and Planetary Science Letters, 278(1–2): 1–12. https://doi.org/10.1016/j.epsl.2008.09.037

Reyes–Harker, A., Montenegro–Buitrago, G. & Gomez, P.D. 2000. Evolucion Tectonoestratigráfica del Valle Inferior del Magdalena, Colombia. VII Simposio Bolivariano de Exploración Petrolera en las Cuencas Subandinas. Memoirs, p. 293–309. Caracas, Venezuela.

Reyes, L., Ortiz, A. & Guzmán, G. 2009. Facial Changes and stratigraphy in the Popa Formation: An example from northern Cartagena, Colombia. X Simposio Bolivariano de Exploración Petrolera en las Cuencas Subandinas. Abstract. Cartagena, Colombia.

Rodríguez–Ramírez, A., Reyes–Nivia, M.C., Zea, S., Navas–Camacho, R., Garzón–Ferreira, J., Bejarano, S., Herrón, P. & Orozco, C. 2010. Recent dynamics and condition of coral reefs in the Colombian Caribbean. Revista de Biología Tropical, 58(suplemento 1): 107–131. https://doi.org/10.15517/RBT.V58I1.20027

Rollins, J.F. 1960. Stratigraphy and structure of the Goajira Peninsula, northwestern Venezuela and northeastern Colombia. Doctoral thesis, University of Nebraska, 151 p. Lincoln, USA.

Rosero, S., Silva, J.C., Sial, A.N., Borrero, C., & Pardo, A. 2014. Quimioestratigrafía de isótopos de estroncio de algunas sucesiones del Eoceno – Mioceno del cinturón de San Jacinto y el Valle Inferior del Magdalena. Boletín de Geología 36(1): p. 15–27.

Salazar–Franco, A.M., Silva–Tamayo, J.C., Bayona, G., Méndez–Duque, J. & Lara, M. 2016. Chemostratigraphy of upper Eocene – lower Oligocene carbonate successions in the Southern Caribbean Margin (San Jacinto deformed belt of Colombia). XII Simposio de Exploración Petrolera en Cuencas Subandias. Abstract, p. 55–56. Bogotá.

Schmidt, D.N. 2007. The closure history of the Central American seaway: Evidence from isotopes and fossils to models and molecules. In: Williams, M., Haywood, A.M., Gregory, F.J. & Schmidt, D.N. (editors), Deep–time perspectives on climate change: Marrying the signal from computer models and biological proxies. The Geological Society of London, p. 427–442. https://doi.org/10.1144/TMS002.19

Silva–Tamayo, J.C., Sierra, G.M. & Correa, L.G. 2008. Tectonic and climate driven fluctuations in the stratigraphic base level of a Cenozoic continental coal basin, northwestern Andes. Journal of South American Earth Sciences, 26(4): 369–382. https://doi.org/10.1016/j.jsames.2008.02.001

Silva–Tamayo, J.C., Lara, M.E., Nana–Yobo, L., Erdal, Y.D. Sanchez, J. & Zapata–Ramirez, P.A. 2017. Tectonic and environmental factors controlling on the evolution of Oligo – Miocene shallow marine carbonate factories along a tropical SE Circum–Caribbean. Journal of South American Earth Sciences, 78: 213–237. https://doi.org/10.1016/j.jsames.2017.06.008

Spooner, E.T.C. 1976. The strontium isotopic composition of seawater, and seawater–oceanic crust interaction. Earth and Planetary Science Letters, 31(1), 167–174. https://doi.org/10.1016/0012-821X(76)90108-4

Swolf, H. 1946. El Difícil Limestone. Ecopetrol, Internal report 007, 90 p. Bogotá.

Thomas, D.J. 1972. The tertiary geology and systematic paleontology (Phylum Mollusca) of the Guajira Peninsula, Colombia, South America. Doctoral thesis. State University of New York at Binhamton, 147 p. New York, USA.

Torres–Lasso, J.C. 2014. Estratigrafía, quimioestratigrafía y petrografía de la Formación Vijes, Valle Del Cauca: Implicaciones para la datación y caracterización de potenciales reservorios carbonáticos en el occidente y Caribe colombiano. Bachelor thesis, Universidad de Caldas, 66 p. Manizales, Colombia.

Tucker, M.E. & Wright, V.P. 1990. Carbonate Sedimentology. Blackwell Scientific Publications, 482 p. London, UK. https://doi.org/10.1002/9781444314175

Tucker, M.E. & Wright, V.P. 2009. Carbonate sedimentology. John Wiley & Sons, 468 p. Chichester, UK.

Vargas–Cuervo, G. 2004. Geología y aspectos geográficos de la isla de San Andrés, Colombia. Geología Colombiana, (29): 73–89.

Villagómez, D., Spikings, R., Magna, T., Kammer, A., Winkler, W. & Beltrán, A. 2011. Geochronology, geochemistry and tectonic evolution of the Western and Central Cordilleras of Colombia. Lithos, 125(3–4): 875–896. https://doi.org/10.1016/j.lithos.2011.05.003

Wickman, F.E. 1948. Isotope ratios: A clue to the age of certain marine sediments. The Journal of Geology, 56(1): 61–66. https://doi.org/10.1086/625478

Wilson, M.E.J. 2002. Cenozoic carbonates in southeast Asia: Implications for equatorial carbonate development. Sedimentary Geology 147(3–4): 295–428. https://doi.org/10.1016/S0037-0738(01)00228-7

Wilson, M.E.J. 2008. Global and regional influences on equatorial shallow–marine carbonates during the Cenozoic. Palaeogeography, Palaeoclimatology, Palaeoecology, 265 (3–4): 262–274. https://doi.org/10.1016/j.palaeo.2008.05.012

Wilson, M.E.J. 2012. Equatorial carbonates: An earth systems approach. Sedimentology, 59(1): 1–31. https://doi.org/10.1111/j.1365-3091.2011.01293.x

Wilson, M.E.J. 2015. Oligo – Miocene variability in carbonate producers and platforms of the Coral Triangle biodiversity hotspot: Habitat mosaics and marine biodiversity. Palaios 30(1): 150–168. https://doi.org/10.2110/palo.2013.135

Zachos, J.C., Pagani, M., Sloan, L., Thomas, E. & Billups, K. 2001. Trends, rhythms, and aberrations in global climate 65 Ma to present. Science, 292(5517): 686–693. https://doi.org/10.1126/science.1059412

Zachos, J.C., Dickens, G.R. & Zeebe, R.E. 2008. An early Cenozoic perspective on greenhouse warming and carbon–cycle dynamics. Nature 451(7176): 279–283. https://doi.org/10.1038/nature06588

Zuluaga, C.A., Ochoa–Yarza, A., Muñoz, C.A., Guerrero, N.M., Martínez, A.M., Medina, P.A., Pinilla, A., Ríos, P.A., Rodríguez, B.P., Salazar, E.A. & Zapata, V.L. 2009. Memoria de las planchas 2, 3, 5 y 6 (con parte de las planchas 4, 10 y 10Bis). Proyecto de investigación: Cartografía e historia geológica de la Alta Guajira. Ingeominas, internal report, 504 p. Bogotá.

Explanation of Acronyms, Abbreviations, and Symbols:

Ecopetrol	Empresa Colombiana de Petróleos S.A.
LBF	Larger benthic foraminifera
NIST	National Institute of Standards and Technology
SJDB	San Jacinto deformed belt

Authors' Biographical Notes

Juan Carlos SILVA–TAMAYO is CEO at Testlab Geambiental–Testlab Laboratorio Análisis Alimentos y Aguas S.A.S. He holds a BS in geology from the EAFIT University Medellín, Colombia, a Master of Science in environmental and sedimentary sciences from the Universidade Federal de Pernambuco, Recife, Brasil, and a PhD in geochemistry from the Universitat Bern, Bern, Switzerland. He was also a Marie Curie Postdoctoral Fellow at the Department of Earth and Environment at Stanford University, USA, and the Department of Earth and Environment at the University of Leeds, UK. His research primarily focuses on sedimentary geology, stratigraphy, and low–temperature isotope geochemistry.

Daniel RINCÓN–MARTÍNEZ, PhD, is a researcher at the Instituto Colombiano del Petróleo of Ecopetrol S.A, Piedecuesta, Colombia. His primary field of research is micropaleontology, particularly benthonic and planktonic foraminifera and its application to paleoceanography, sequence stratigraphy, and paleoecology. His research projects encompass rocks formed in a wide variety of depositional environments (marginal, shallow, and deep marine) and ages (Mesozoic to Neogene). In recent years, RINCÓN–MARTÍNEZ has focused attention on Paleogene shallow–marine carbonate systems and compared them to basinal pelagic records for regional analysis of southern Caribbean geology.

Lina M. BARRIOS is a marine biologist with PhD in marine ecology (two main thesis topics: connectivity and proxy indicators of climate change). Her main area of work is the population and community ecology (ecological genetics) of tropical marine organisms, including conservation biology and biodiversity. Most of her work involves international and multithematic groups around the world (e.g., tropical eastern Pacific, Caribbean, North Sea, Mediterranean Sea, and China Sea). Since 2003, she has worked on comparative ecology (tropical vs. temperate environments) as a lecturer and researcher. Her research has taken her into fascinating questions regarding coral connectivity and gene expression under climate change–ocean acidification scenarios (https://www.ecologicalgenetics.org/lina-barrios-gardelis).

Juan C. TORRES–LASSO holds a master's degree in physical, chemical, and geological oceanography from the Federal University of Rio Grande in Brazil. The main research interests of TORRES–LASSO focus on physical and chemical oceanography as well as on the investigation of the evolution of reefal calcareous organisms through geological time, on the quantification of the dependency of reef formation on climatic variations, and on the constraints of ocean physicochemical characteristics that affect calcareous organisms, making them adapt to these changes. Currently, he is working at the Instituto de Investigaciones Marinas y Costeras (Invemar) in Colombia.

Chixel OSORIO–ARANGO is a geologic engineer from the Universidad Nacional de Colombia. She has worked on several projects related to sedimentary geology and stratigraphy, and on the exploration of clay minerals that can be used as biocide agents. She currently works as an independent consultant.